Cellular/Molecular

Inducible CRISPR Epigenome Systems Mimic Cocaine Induced Bidirectional Regulation of Nab2 and Egr3

Eric Y. Choi,[1,2] Daniela Franco,[1,3] Catherine A. Stapf,[1,3] Madeleine Gordin,[1] Amanda Chow,[1] Kara K. Cover,[1,3] Ramesh Chandra,[1,4] and Mary Kay Lobo[1]

[1]Department of Anatomy and Neurobiology, [2]Graduate Program in Life Sciences, Biochemistry and Molecular Biology, [3]Program in Neuroscience, Graduate Program in Life Sciences, and [4]Center for Innovative Biomedical Resources, Virus Vector Core, University of Maryland School of Medicine Baltimore, Maryland, 21201

Substance use disorder is a chronic disease and a leading cause of disability around the world. The NAc is a major brain hub mediating reward behavior. Studies demonstrate exposure to cocaine is associated with molecular and functional imbalance in NAc medium spiny neuron subtypes (MSNs), dopamine receptor 1 and 2 enriched D1-MSNs and D2-MSNs. We previously reported repeated cocaine exposure induced transcription factor early growth response 3 (*Egr3*) mRNA in NAc D1-MSNs, and reduced it in D2-MSNs. Here, we report our findings of repeated cocaine exposure in male mice inducing MSN subtype-specific bidirectional expression of the *Egr3* corepressor NGFI-A-binding protein 2 (*Nab2*). Using CRISPR activation and interference (CRISPRa and CRISPRi) tools combined with *Nab2* or *Egr3*-targeted sgRNAs, we mimicked these bidirectional changes in Neuro2a cells. Furthermore, we investigated D1-MSN- and D2-MSN-specific expressional changes of histone lysine demethylases *Kdm1a*, *Kdm6a*, and *Kdm5c* in NAc after repeated cocaine exposure in male mice. Since *Kdm1a* showed bidirectional expression patterns in D1-MSNs and D2-MSNs, like *Egr3*, we developed a light-inducible Opto-CRISPR-KDM1a system. We were able to downregulate *Egr3* and *Nab2* transcripts in Neuro2A cells and cause similar bidirectional expression changes we observed in D1-MSNs and D2-MSNs of mouse repeated cocaine exposure model. Contrastingly, our Opto-CRISPR-p300 activation system induced the *Egr3* and *Nab2* transcripts and caused opposite bidirectional transcription regulations. Our study sheds light on the expression patterns of *Nab2* and *Egr3* in specific NAc MSNs in cocaine action and uses CRISPR tools to further mimic these expression patterns.

Key words: **addiction; cocaine; CRISPR; drug; *Egr3*; *Nab2***

Significance Statement

Substance use disorder is a major societal issue. The lack of medication to treat cocaine addiction desperately calls for a treatment development based on precise understanding of molecular mechanisms underlying cocaine addiction. In this study, we show that *Egr3* and *Nab2* are bidirectionally regulated in mouse NAc D1-MSNs and D2-MSNs after repeated exposure to cocaine. Furthermore, histone lysine demethylations enzymes with putative EGR3 binding sites showed bidirectional regulation in D1- and D2-MSNs after repeated exposure to cocaine. Using Cre- and light-inducible CRISPR tools, we show that we can mimic this bidirectional regulation of *Egr3* and *Nab2* in Neuro2a cells.

Introduction

The nucleus accumbens (NAc) or ventral striatum is a major brain hub that is critical for reward behaviors (Di Chiara, 2002; Wise, 2004; Russo and Nestler, 2013; Salgado and Kaplitt, 2015). Dopamine D1 receptor or D2 receptor-expressing medium spiny neurons (MSNs) of the NAc project to differential outputs through the brain to constitute both the reward and ventral basal ganglia circuits (Gerfen et al., 1990; Smith et al., 2013). Previous studies demonstrate opposing roles for these two MSN subtypes in behavioral responses to psychostimulants, but the landscape of molecular changes and functional imbalance within these MSNs continues to be uncovered (Hikida et al., 2010; Lobo et al., 2010; Ferguson et

Received Sep. 19, 2022; revised Dec. 6, 2022; accepted Dec. 22, 2022.

Author contributions: E.Y.C., R.C., and M.K.L. designed research; E.Y.C., C.A.S., M.G., A.C., K.K.C., and R.C. performed research; E.Y.C., D.F., R.C., and M.K.L. analyzed data; E.Y.C. and D.F. wrote the first draft of the paper; E.Y.C. and M.K.L. edited the paper; E.Y.C. and M.K.L. wrote the paper.

This work was supported by the National Institutes of Health Grants R21 DA046227, R21 DA052101, and R01 DA038613 to M.K.L. and F31 DA052967 to E.Y.C. We thank Alexandros Poulopoulos, Ryan Richardson, Thomas A. Blanpied, and Aaron D. Levy (University of Maryland School of Medicine) for advice and shared resources for Light Plate Apparatus experiments.

The authors declare no competing financial interests.

Correspondence should be addressed to Ramesh Chandra at rchandra@som.umaryland.edu or Mary Kay Lobo at mklobo@som.umaryland.edu.

https://doi.org/10.1523/JNEUROSCI.1802-22.2022

al., 2011; Lobo and Nestler, 2011; Bock et al., 2013; Chandra et al., 2013; Lenz and Lobo, 2013; Engeln et al., 2020). Processes that mediate psychostimulant-induced altered transcriptional landscapes in MSN subtypes can occur through an imbalance in molecular signaling cascades, transcription factors, and epigenetic modifications of chromatin in MSNs (Lee et al., 2006; Bateup et al., 2008; Lobo et al., 2010, 2013; Lobo and Nestler, 2011; Chandra et al., 2013). This is supported by studies which demonstrate that these processes in each MSN subtype lead to differential regulation of transcription, synaptic plasticity, and behavioral responses to psychostimulants (Bateup et al., 2010; Lobo et al., 2010; Lobo and Nestler, 2011; Arango-Lievano et al., 2014; Maze et al., 2014; Chandra et al., 2015, 2017a,b; Engeln et al., 2020, 2022; Cole et al., 2021).

Dysregulation of dopamine (DA) and brain-derived neurotrophic factor (BDNF) signaling in the NAc are induced by repeated psychostimulant exposure, resulting in altered gene expression for synaptic and behavioral plasticity geared toward repeated drug intake and seeking (Hyman et al., 2006; Russo et al., 2009; Volkow et al., 2009; McGinty et al., 2010). Here, we investigated a key molecular target of both DA and BDNF signaling, the transcription factor early growth response 3 *(Egr3*), and its corepressor NGFI-A binding protein 2 *(Nab2*) (Patwardhan et al., 1991; Yamagata et al., 1994; O'Donovan and Baraban, 1999; Jouvert et al., 2002; Roberts et al., 2006). Previous studies demonstrate that *Egr3* is important for the induction of cellular programs of differentiation, proliferation, and cell death in response to environmental stimuli that rapidly and transiently induces its expression (Thiel and Cibelli, 2002; Unoki and Nakamura, 2003; Carter et al., 2007). NAB2 can modulate the activity of EGR3 by binding with EGR3 and engaging corepressor functions (Kumbrink et al., 2010). EGR3 can also bind to the *Nab2* promoter and activate *Nab2* transcription, thereby repressing EGR3 through a negative feedback loop (Kumbrink et al., 2005, 2010). Notably, the expression patterns of EGR3 and NAB2 are shown to be variable depending on different cell types and stimuli (Beckmann and Wilce, 1997; Honkaniemi et al., 2000; Collins et al., 2008).

In recent years, the development of epigenetic modification tools and CRISPR tools allowed neuroscientists to alter gene expression at specific gene loci with greater specificity compared with traditional RNAi-based silencing or cDNA-based overexpression (Qi et al., 2013; Heller et al., 2014, 2016; Ran et al., 2015; Farhang et al., 2017; Klann et al., 2017; Savell et al., 2019; Duke et al., 2020; Eagle et al., 2020; Teague et al., 2022). Additionally, previous studies used transcription activator-like effectors (TALE) for epigenetic editing and light-inducible epigenetic editing (Konermann et al., 2013). However, the complex and lengthy procedures of TALE engineering make CRISPR approaches more favorable. Here, we use D1-Cre- and D2-Cre-specific RiboTag mice (Gong et al., 2007; Sanz et al., 2009, 2013; Gerfen et al., 2013; Chandra et al., 2015) to further explore *Nab2* and other *Egr3* targets in MSN subtypes after repeated cocaine exposure and use these CRISPR tools in Neuro2A cells to explore *Egr3* and *Nab2* dynamics.

Materials and Methods

Mice. WT C57BL/6J mice were purchased from The Jackson Laboratory and used for chromatin immunoprecipitation (ChIP) experiments. Homozygous RiboTag (RT) mice on a C57BL/6J background expressing a Cre-inducible HA-Rpl22 were purchased from The Jackson Laboratory. *D1-Cre* hemizygote (line FK150) and *D2-Cre* hemizygote (line ER44) BAC transgenic mice from GENSAT on C57BL/6J background were crossed with RT mice to generate *D1-Cre-RT* and *D2-Cre-RT* mice and used for cell type-specific isolation of ribosome-associated mRNA. All mice used for experiments were maintained on a 12 h light/dark cycle with *ad libitum* access to food and water. All experiments were conducted in accordance with the guidelines set up by the Institutional Animal Care and Use Committee at the University of Maryland School of Medicine.

Repeated cocaine treatment. Male *D1-C.re-RT*, *D2-Cre-RT* and C57BL/6J WT mice received 7 daily intraperitoneal injections of cocaine (20 mg/kg) or 0.9% saline in the home cage. NAc tissue punches were collected 24 h after the last injection for molecular biology experiments or cross-linked in 1% formaldehyde for ChIP experiments. Cocaine hydrochloride (Sigma) was dissolved in sterile saline. The dose of cocaine and the 24 h abstinent time point was selected based on previous studies showing important cocaine-mediated transcriptional and plasticity changes at the time point (Maze et al., 2010; Russo et al., 2010; Kim et al., 2011; Feng et al., 2014).

Cell culture transfection. Neuro2A cell cultures were maintained in DMEM supplemented with 10% FBS and penicillin/streptomycin (all from Fisher Scientific). Cell cultures of passage number between 5 and 10 were used for the entire experiment. Twenty-four hours before transfection, cells were seeded at the density of 1.5×10^5 cells per well in 24 well plates. Transfection was performed using Invitrogen LF3000 reagents following the manufacturer's standard protocol. Six hours after the start of transfection, cells received fresh media change with DMEM supplemented with 10% FBS and penicillin/streptomycin. For CRISPR activation (CRISPRa) or CRISPR interference (CRISPRi) experiments, cells were harvested 48 h after transfection for RNA, protein, or Cut&Run sample preparation. For Opto-CRISPRa and Opto-CRISPRi experiments, cells received light stimulation 48 h after transfection, and harvested 1 h after light stimulation for RNA sample, 4 h after light stimulation for protein sample, or immediately for Cut&Run sample.

Opto-CRISPR light stimulation. A custom-built 24 well light plate apparatus with 460 nm LED bulbs set to emit 1 mW of light was used for light stimulation (Gerhardt et al., 2016). On the day of light stimulation (48 h after transfection), cells plated on 24 well plates received media change to colorless BrightCell NEUMO Photostable media (EMD Millipore SCM146-1) supplemented with 1× BrightCell SOS Neuronal Supplement (EMD Millipore SCM147-1) and 1% penicillin/streptomycin at least 3 h before the start of light stimulation to avoid blue light-induced gene alterations (Duke et al., 2019). Two hours of steady-state light stimulation iris protocol was loaded onto the light plate apparatus (http://taborlab.github.io/Iris/). The 24 well plates with transfected cells were inserted into the light plate apparatus and placed back into the cell incubator set at 37°C and 5% CO_2 level for 2 h light stimulation. After 2 h of light stimulation, the cells remained in the incubator and was harvested 1 h after light stimulation for RNA samples, 4 h after light stimulation for protein samples, or immediately for Cut&Run samples.

Western blotting. Cell lysates were prepared with RIPA buffer (Sigma-Aldrich R0278) supplemented with Phosphatase Inhibitor Cocktail 2 (Sigma-Aldrich P5726), Phosphatase Inhibitor Cocktail 3 (Sigma-Aldrich P0044), and Complete Protease Inhibitor Cocktail (Roche 11873580001). Electrophoresis was performed using Mini-Protean TGX Gels (Bio-Rad 4569033) followed by the transfer onto a nitrocellulose membrane (Bio-Rad 1620094). After blocking in 5% skim milk/TBS supplemented with 0.1% Tween 20 (TBST), membranes were incubated with primary antibody overnight at 4°C followed by secondary antibody incubation for 1 h at room temperature. Blot images were captured using Bio-Rad ChemiDoc MP Imager, and the raw band intensities were quantified relative to GAPDH band intensities using ImageJ (National Institutes of Health). For Opto-CRISPR-KDM1A and Opto-CRISPR-p300 Western blot quantification analyses, GAPDH normalized NAB2 band intensities from 2 h light stimulation samples were normalized to GAPDH normalized NAB2 band intensities from no light stimulation control samples. Consistently, GAPDH normalized EGR3 band intensities from 2 h light stimulation samples were normalized to GAPDH normalized EGR3 band intensities from no light stimulation control samples. The

following primary antibodies were used at 1:1000 dilution: NAB2 (Santa Cruz Biotechnology SC-22 815), EGR3 (Santa Cruz Biotechnology SC-191), and GAPDH (Cell Signaling 2118s).

ChIP. Fresh NAc punches were prepared for ChIP as described previously (Chandra et al., 2015). Briefly, four 14 NAc punches per animal (5 male mice pooled per sample) were collected, cross-linked with 1% formaldehyde, and quenched with 2 M glycine before being flash frozen on dry ice and stored in −80°C. Before sample sonication, IgG magnetic beads (Invitrogen; Sheep anti-rabbit 11202D) were incubated in blocking solution (0.5% BSA in PBS) which contains 15 μg of anti-Nab2 antibody (Santa Cruz Biotechnology SC22815) per reaction at 4°C overnight under constant rotation. NAc tissues were Dounce homogenized in 1 ml lysis buffer (50 mM HEPES-KOH, pH 7.5, 140 mM NaCl, 1 mM EDTA, 10% glycerol, 0.5% NP-40, 0.25% Triton X-100, and protease inhibitors) and placed on rotator at 4°C for 10 min. Samples were centrifuged at 1350 × *g* for 5 min at 4°C, and the pellet was resuspended in 1 ml of lysis buffer 2 (10 mM Tris-HCl, pH 8.0, 200 mM NaCl, 1 mM EDTA, 0.5 mM EGTA, and protease inhibitors) and incubated gently on shaker at room temperature for 10 min. Then, nuclei were pelleted by centrifugation at 1350 × *g* for 5 min at 4°C and resuspended in 300 μl of lysis buffer 3 (10 mM Tris-HCl, pH 8.0, 100 mM NaCl, 1 mM EDTA, 0.5 mM EGTA, 0.1% Na-deoxycholate, 0.5% *N*-lauroylsarcosine, and protease inhibitors). Chromatins were sheared to an average length of 500-700 bp by the Diagenode Bioruptor Pico Sonicator using eight cycles of 30 s on and off at 4°C. Then, 1/10 volume of 10% Triton X-100 was added to the sonicated lysate to permeate the nuclear membrane. Samples were centrifuged at 20,000 × *g* for 10 min at 4°C to pellet the debris. After washing and resuspension of the antibody bead conjugates, the mixtures were added to each chromatin sample and incubated for 16 h under constant rotation at 4°C. Samples were then washed on magnetic stands and reverse cross-linked at 65°C overnight. Chromatin was purified using a PCR purification kit (QIAGEN 28 104) and used for qPCR analysis normalized to their respective input controls as previously described.

Cut&Run. Neuro2a cells were harvested 48 h after transfection for CRISPRa and CRISPRi experiments, flash frozen on dry ice, and stored at −80°C. For Opto-CRISPRa and Opto-CRISPRi experiments, Neuro2a cells were harvested immediately after light stimulation, flash frozen on dry ice, and stored at −80°C. Cut&Run experiment was performed using Cell Signaling Cut&Run Kit (86652) following the manufacturer's standard protocol. Cells were homogenized in 1 ml Dounce homogenizer, 20 ups and downs using pestle A, and then another 20 ups and downs using pestle B, in wash buffer supplemented with spermidine and protease inhibitor cocktail according to the manufacturer's recipe. Enriched chromatins were purified using Cell Signaling ChIP and Cut&Run DNA Purification Kit (14209) following the manufacturer's standard protocol. The following antibodies were used at 2 μl per sample for negative control and 5 μl per sample for all remaining antibodies: Normal Rabbit IgG (Cell Signaling 66 362), H3K4me3 (Cell Signaling 9751), H3K27AC (Cell Signaling 8173), and HA (Cell Signaling 3724).

Polyribosome immunoprecipitation and RNA isolation. Immunoprecipitation of polyribosome was prepared from NAc of male *D1-Cre-RT* and *D2-Cre-RT* mice according to our previous study (Chandra et al., 2015). In brief, four 14-gauge NAc punches per animal (4 animals pooled per sample) were collected and homogenized by douncing in homogenization buffer; 800 μl of the homogenate was added directly to the HA-coupled magnetic beads (Invitrogen: 100.03D; Covance: MMS-101R) for constant rotation overnight at 4°C. The following day, beads were washed 3 times in high-salt buffer using a magnetic stand. Finally, RNA was extracted using the MicroElute Total RNA Kit (Omega) according to the manufacturer's standard protocols. RNA was quantified with a NanoDrop (Thermo Scientific).

RNA extraction and cDNA synthesis. RNA extraction samples were prepared from Neuro2a cells using QIAGEN RNeasy micro plus kit (QIAGEN 74034). Neuro2a cells were harvested directly from the wells with application of Buffer RLT and physical scraping using a cell scraper. The cell lysate then underwent a series of affinity column-based extraction and purification following the manufacturer's standard protocol. Purified RNA samples were quantified, and 500 ng cDNA samples were synthesized using Bio-Rad iScript cDNA synthesis kit following the manufacturer's standard protocol (Bio-Rad 1708891). Synthesized cDNA samples were diluted 10 folds and stored in −20°C.

qPCR analysis. qRT-PCR and Cut&Run qPCR experiments were conducted with PerfeCTa SYBR Green FastMIX (Quantabio 95072-012) on Bio-Rad CFX384 Real-Time Thermal Cycler. Gene-specific primer sets were obtained from MGH PrimerBank (https://pga.mgh.harvard.edu/primerbank/) or designed using NCBI Primer BLAST (https://www.ncbi.nlm.nih.gov/tools/primer-blast/). The primer sequences used in the experiments are as follows: *Nab2* primer forward, CATTCTCCAT CCTTGCACTCG; *Nab2* primer reverse, CCCTGCCTGTTATTGCT TGA; *Egr3* primer forward, CCGGTGACCATGAGCAGTT; *Egr3* primer reverse, TAATGGGCTACCGAGTCGC; *Nab2* Cut&Run primer forward, CCGGTTCTGCCCACGCCCTC; *Nab2* Cut&Run primer reverse, TCC ACCGCTGTCCAGGCTCC; *Egr3* Cut&Run primer forward, GCTGC ACGTTGGCTGCGG; *Egr3* Cut&Run primer reverse, CCTAGCTAGC TCACTGCTGCC; *Nab2* ChIP primer 1 forward, CGCCAGGCAAAG AGCAGCGC; *Nab2* ChIP primer 1 reverse, CGGAGTCCAACTCC ACCCATCT; *Nab2* ChIP primer 2 forward, GGGGTCTAAAGGGTG GAGGTCG; *Nab2* ChIP primer 2 reverse, CAGGGGGCTCATGTG CCAGGT.

Immunocytochemistry. Neuro2a cells plated on glass coverslips were fixed in 4% PFA for 30 min and then washed with PBS. The coverslips were then placed in blocking solution (PBS supplemented with 2% normal donkey serum, 1% BSA, 0.1% Triton X-100, 0.05% Tween 20, and 0.05% sodium azide) for 1 h at room temperature and then incubated at 4°C overnight with the following primary antibodies: chicken anti-GFP (1:5000, Aves Labs GFP-1020), mouse anti-HA tag (1:400, Abcam ab18181), and rabbit anti-FLAG tag (1:400, Sigma F7425). After series of washing with PBS, the coverslips were incubated with fluorophore-conjugated secondary antibodies at 1:400 dilution for either 2 h at room temperature or at 4°C overnight. Following another series of washing with PBS, the coverslips were mounted on glass slides with DAPI containing Vectashield mounting medium (Vector Laboratories H-1200). *Z*-stack images were acquired with Leica SP8 confocal microscope and then processed on ImageJ (National Institutes of Health).

Constructs. Cre-inducible pAAV-EF1a-DIO-dSaCas9-CIBN-HA vector and pAAV-EF1a-DIO-Cry2-KDM1A-FLAG vector were commercially made from VectorBuilder. pAAV-EF1a-DIO-Cry2-p300core-FLAG vector was made by taking out KDM1A sequence out of the pAAV-EF1a-DIO-Cry2-KDM1A-FLAG vector using the restriction sites EcoRI and NotI, and cloning in p300core insert fragment into the EcoRI and NotI sites. pAAV-EF1a-DIO-dSaCas9-VP64-HA vector and pAAV-EF1a-DIO-dSaCas9-KRAB-HA were made by taking out CIBN sequence out of the pAAV-EF1a-DIO-dSaCas9-CIBN-HA vector using the restriction sites EcoRI and NotI, and cloning in VP64 or KRAB insert fragments into the EcoRI and NotI sites. sgRNA vectors with an independent Cre-inducible EGFP reporter were designed using PX552 vector gifted from Feng Zhang Lab (Addgene plasmid #60958; http://n2t.net/addgene:60958; RRID:Addgene_60958). Conventional EGFP sequence in the original vector was taken out using the restriction sites SalI and EcoRI and replaced with DIO-NLS-EGFP sequence using the same SalI and EcoRI sites. The sequences of all the vector used in this study were confirmed by conventional Sanger sequencing.

Statistical analysis. Student's *t* test and one-way ANOVA were used with $p < 0.05$ considered statistically significant. For multiple testing corrections, Tukey's *post hoc* test was used as indicated in Results. All the statistical analyses were performed with GraphPad Prism 6 (GraphPad Software).

Results

Nab2 is bidirectionally regulated in NAc D1-MSNs versus D2-MSNs after repeated exposure to cocaine

We first investigated the regulation of *Nab2* expression in the NAc after seven daily injections of cocaine (20 mg/kg) followed by a 24 h abstinent period, which is a critical time point for transcriptional and plasticity changes occurring in the NAc as

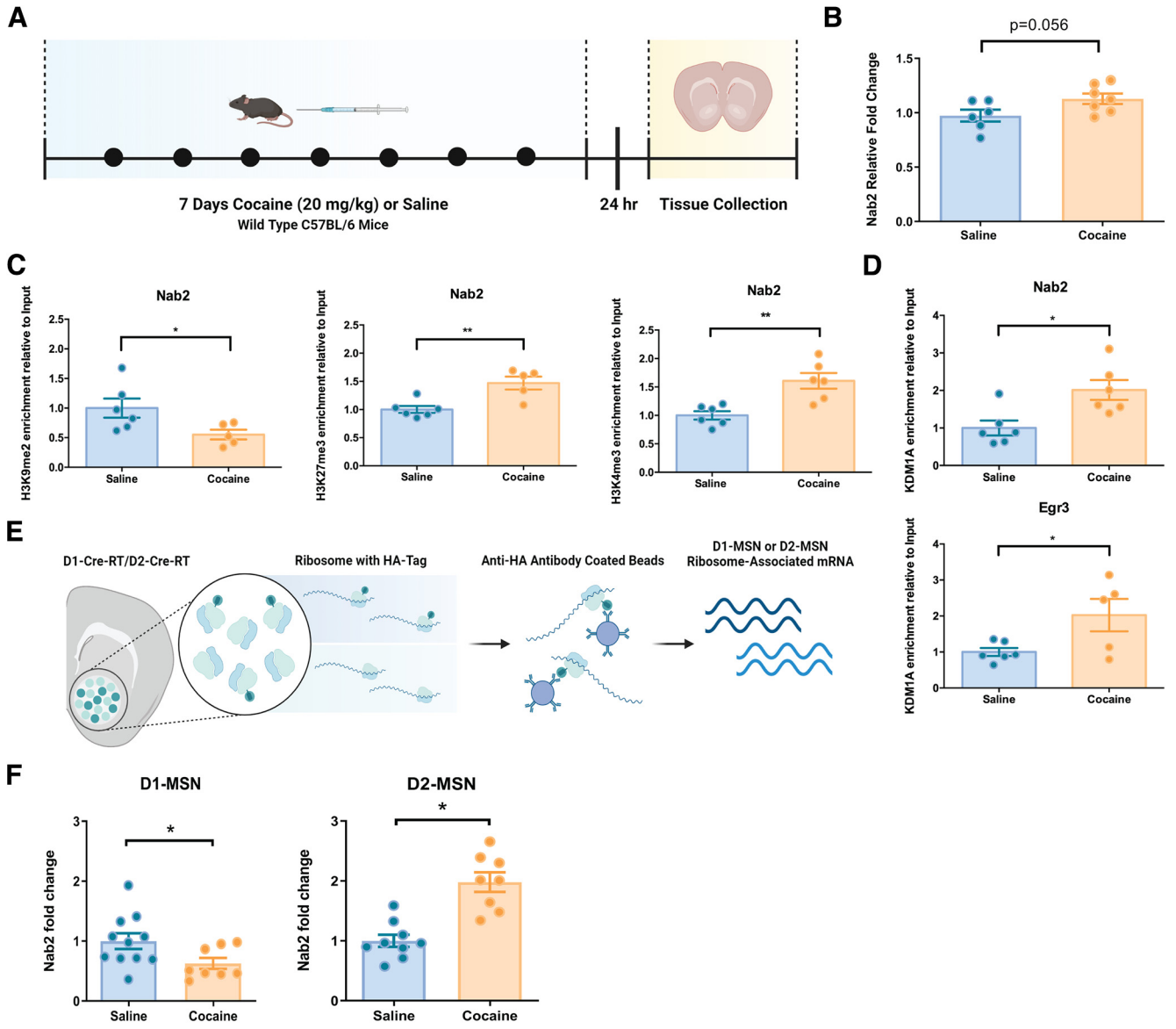

Figure 1. *Nab2* ribosome-associated mRNA expression after repeated cocaine exposure. ***A***, Male mice received intraperitoneal injection of cocaine (20 mg/kg) for 7 consecutive days. NAc punches were harvested 24 h after last cocaine injection. ***B***, qRT-PCR analysis shows a trend toward an increase in *Nab2* mRNA expression in the NAc after repeated cocaine exposure in male mice (saline $n = 6$, cocaine $n = 7$). ***C***, Transcription repression associated H3K9me2 and H3K27me3 marks show bidirectional enrichment on *Nab2* promoter after repeated exposure to cocaine. A transcription activation associated H3K4me3 mark showed an increased enrichment on *Nab2* promoter after repeated exposure to cocaine (H3K4me3 saline $n = 6$, cocaine $n = 6$; H3K9me2 saline $n = 6$, cocaine $n = 5$; H3K27me3 saline $n = 6$, cocaine $n = 5$). ***D***, Histone demethylase KDM1A showed an increased enrichment on both *Nab2* and *Egr3* promoters after repeated exposure to cocaine (*Nab2* saline $n = 6$, cocaine $n = 6$; *Egr3* saline $n = 6$, cocaine $n = 5$). ***E***, *D1-Cre-RT* and *D2-Cre-RT* mice allow cell subtype specific isolation of ribosome associated mRNA. ***F***, Repeated cocaine exposure reduced *Nab2* mRNA expression in D1-MSNs while inducing *Nab2* mRNA expression in D2-MSNs (D1-MSNs saline $n = 11$, cocaine $n = 8$; D2-MSNs saline $n = 9$, cocaine $n = 8$). Each bar represents mean ± SEM. $^{*}p < 0.05$, $^{**}p < 0.01$.

previously reported (Fig. 1*A*) (Maze et al., 2010; Russo et al., 2010; Kim et al., 2011; Feng et al., 2014; Chandra et al., 2015, 2017a,b). Using qRT-PCR, we did not observe a statistically significant change in *Nab2* mRNA expression; however, there was a trend toward an increase in *Nab2* mRNA expression after repeated cocaine in bulk NAc (Student's *t* test, $p = 0.056$; mRNA $n = 6$ or 7 per group, $t_{(10)} = 2.133$, $p < 0.05$; Fig. 1*B*). Next, we performed ChIP to examine hallmark activation and repressive histone methylation modifications on lysine residues, H3K9me2, H3K27me3, and H3K4me3 (Shi et al., 2004; Wysocka et al., 2006; Robison and Nestler, 2011; Ferrari et al., 2014; Nestler, 2014) on the *Nab2* promoter. Interestingly, we observed that repression-associated H3K9me2 and H3K27me3 modifications on *Nab2* promoter were bidirectionally regulated in the NAc. H3K9me2 enrichment was decreased while H3K27me3 enrichment was increased on the *Nab2* promoter in the NAc after repeated exposure to cocaine compared with saline control mice (Student's *t* test, $^{*}p < 0.05$, $^{**}p < 0.01$; pooled ChIP sample $n = 5$ or 6 per group, $t_{(9)} = 2.309$, $p < 0.05$; pooled ChIP sample $n = 5$ or 6 per group, $t_{(9)} = 3.774$, $p < 0.05$; Fig. 1*C*). Furthermore, we saw an increase in activation-associated H3K4me3 modification on *Nab2* chromatin after repeated exposure to cocaine compared with saline controls (Student's *t* test, $^{**}p < 0.01$; pooled ChIP sample $n = 6$ per group, $t_{(10)} = 3.903$, $p < 0.05$; Fig. 1*C*). We also examined the enrichment of histone demethylase KDM1A, which was previously reported to induce demethylation at H3K4 and H3K9 (Shi et al., 2004; Metzger et al., 2005; Rudolph et al., 2013), on both *Nab2* and *Egr3*

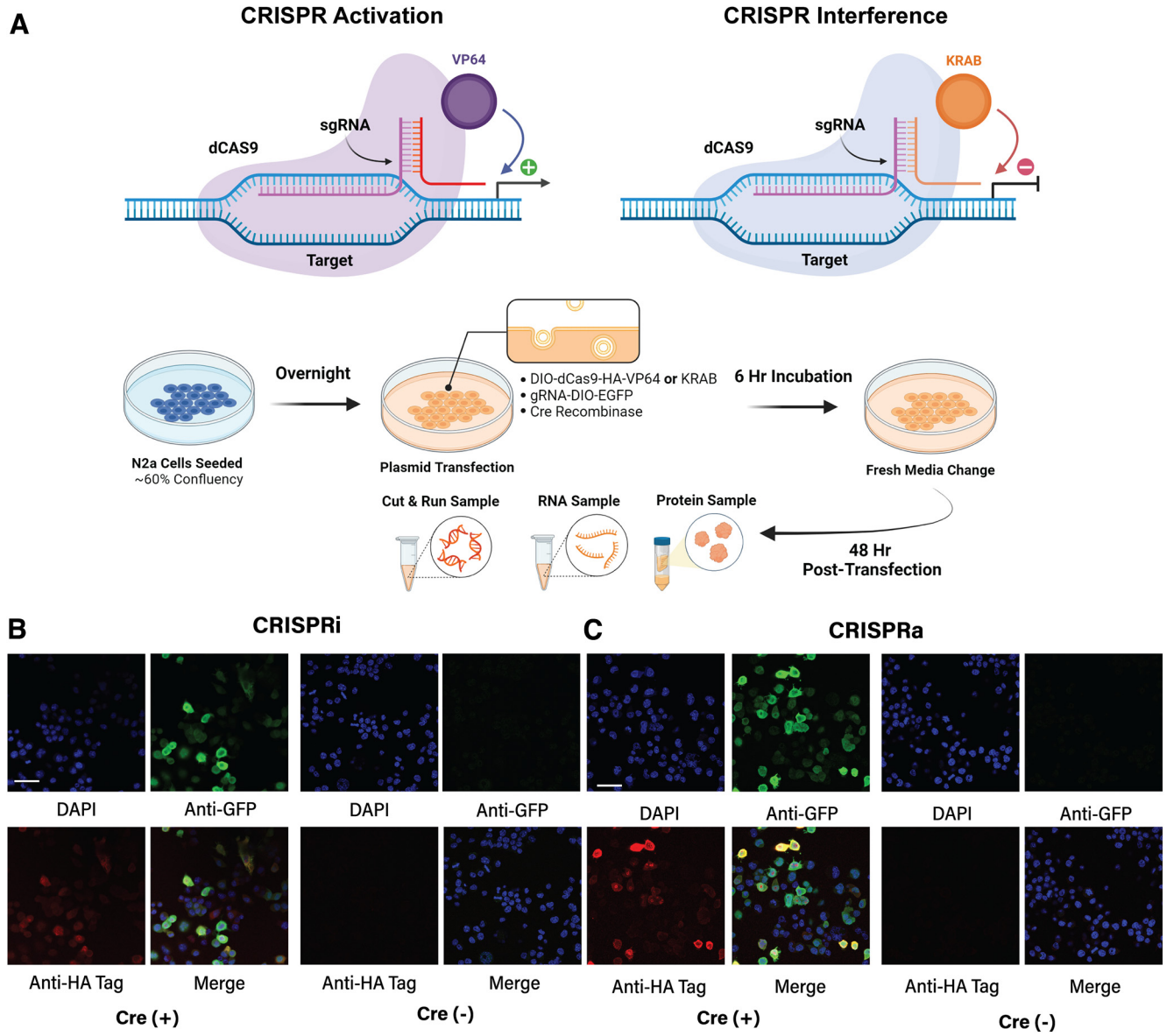

Figure 2. Cell subtype-specific CRISPRa transcriptional activation and CRISPRi transcriptional interference. ***A***, Illustration of a Cre recombinase-dependent expression of a catalytically dead saCas9 fused with VP64 or KRAB in Neuro2a cell line. Transfected cells are harvested 48 h after transfection. ***B***, ***C***, Immunocytochemistry of Neuro2a cells transfected with CRISPRi and CRISPRa systems displays a Cre-inducible expression as observed by GFP (green) and HA-Tag (red) expression. Blue represents DAPI signal. Scale bar, 50 μm.

promoters. We observed increase in the enrichment of KDM1A on both *Nab2* and *Egr3* promoters (Student's *t* test, $^*p < 0.05$; pooled ChIP sample $n = 6$ per group, $t_{(10)} = 3.070$, $p < 0.05$; pooled ChIP sample $n = 5$ or 6 per group, $t_{(9)} = 2.410$, $p < 0.05$; Fig. 1*D*). These complex and bidirectional findings of transcriptional regulation of *Nab2* in the heterogeneous NAc suggested a need for cell subtype-specific analysis to elucidate *Nab2* dynamics in cocaine action.

Using a Cre-inducible RiboTag mouse line crossed with D1 Cre and D2 Cre mouse lines, we generated mouses lines with D1- or D2-MSN-specific expression of ribosomal subunit Rpl22 labeled with hemagglutinin (HA) protein which allow cell subtype-specific polyribosome immunoprecipitation with an HA antibody (*D1-Cre-RT* and *D2-Cre-RT*). These mouse lines and similar approaches allow isolation of ribosome-associated mRNA from each MSN subtype (Fig. 1*E*) (Lobo et al., 2006; Heiman et al., 2008; Ena et al., 2013; Rothwell et al., 2014; Chandra et al., 2015). Seven daily injections of cocaine (20 mg/kg) followed by 24 h of abstinent period resulted in reduced *Nab2* mRNA expression in D1-MSNs while inducing it in D2-MSNs (Student's *t* test, $^*p < 0.05$; pooled ChIP sample $n = 8$-11 per group, $t_{(17)} = 2.156$, $p < 0.05$; pooled ChIP sample $n = 8$ or 9 per group, $t_{(15)} = 5.195$, $p < 0.05$; Fig. 1*F*). Notably, the mRNA expression patterns of *Nab2* in D1 and D2-MSNs were in the opposite direction to our previously reported mRNA expression patterns of *Egr3* (Chandra et al., 2015).

CRISPRi- and CRISPRa-induced perturbation of *Nab2* and *Egr3* expression mimics cocaine-induced bidirectional regulation of these transcripts

We next adopted a CRISPRi or CRISPR activation (CRISPRa) system in Neuro2a cells to determine whether we can recapitulate the cocaine-induced *Egr3* and *Nab2* transcriptional regulation observed with repeated cocaine in NAc cell types. We transfected Neuro2a cells with Cre-inducible DIO-dCas9-KRAB-HA (CRISPRi) or DIO-dCas9-VP64-HA (CRISPRa), an sgRNA

targeting *Egr3*, *Nab2*, or lacZ promoters with an EGFP reporter, and Cre-recombinase (Fig. 2*A*). This system allows the flexibility to freely exchange sgRNA vectors for different gene targets and allows targeting to Cre-expressing cells. To validate the Cre-induced expression of our vectors, we performed immunocytochemistry on Neuro2a cells transfected with CRISPRi and lacZ targeting sgRNA with or without Cre recombinase vector. Forty-eight hours after transfection, samples were fixed and immunostained with anti-GFP, anti-HA, and DAPI was labeled. We observed GFP and HA signals only in Cre-positive cells (Fig. 2*B*). In Cre-negative cells, we did not observe signals from GFP and HA staining but only observed DAPI signals (Fig. 2*B*). We performed the same experiment with the CRISPRa and lacZ targeting sgRNA with or without Cre recombinase vector. Consistent with our results using CRISPRi, we only observed GFP and HA signals from Cre-positive cells (Fig. 2*C*).

To determine whether we can use CRISPRi and CRISPRa systems to target *Nab2* and *Egr3*, we designed sgRNAs against *Nab2* and *Egr3*. For *Nab2* sgRNAs, two ideal spacer sequences followed by NGRRN PAM sequence were identified 363 and 729 bp upstream of the *Nab2* transcription start site (Ran et al., 2015). *Egr3* sgRNA was designed in a similar manner with ideal spacer sequence 567 bp upstream of the *Egr3* transcription start site. Neuro2a cells transfected with *Nab2* sgRNAs and CRISPRi displayed significant reduction of *Nab2* mRNA expression, while *Egr3* mRNA was upregulated compared with lacZ sgRNA controls (one-way ANOVA, *Nab2*: interaction $F_{(3,32)} = 30.46$; $p < 0.0001$, Tukey post-test: $^{*}p < 0.05$, $^{**}p < 0.01$, $^{****}p < 0.0001$; *Egr3*: interaction $F_{(3,32)} = 15.74$; $p < 0.0001$, Tukey post-test: $^{*}p < 0.05$, $^{**}p < 0.01$; mRNA $n = 9$ per group; Fig. 3*A*). In cells transfected with *Egr3* sgRNA and CRISPRi, we observed reduction of *Egr3* mRNA and upregulation of *Nab2* mRNA compared with lacZ sgRNA controls (one-way ANOVA, *Nab2*: interaction $F_{(3,32)} = 30.46$; $p < 0.01$, Tukey post-test: $^{*}p < 0.05$, $^{**}p < 0.01$, $^{****}p < 0.0001$; *Egr3*: interaction $F_{(3,32)} = 15.74$; $p < 0.01$, Tukey post-test: $^{*}p < 0.05$, $^{**}p < 0.01$; mRNA $n = 9$ per group; Fig. 3*A*). These data are consistent with the bidirectional regulation of *Nab2* and *Egr3* that we observed in NAc cell types after repeated cocaine exposure. Using CRISPRa with *Nab2* or *Egr3* sgRNAs, we successfully activated *Nab2* or *Egr3* mRNA with their respective sgRNAs compared with lacZ sgRNA control (one-way ANOVA, *Nab2*: interaction $F_{(3,32)} = 10.35$; $p < 0.0001$, Tukey post-test: $^{**}p < 0.01$. *Egr3*: interaction $F_{(3,32)} = 5.848$; $p < 0.01$, Tukey post -test: $^{**}p < 0.01$; mRNA $n = 9$ per group; Fig. 3*B*). With each sgRNA and CRISPRa, we did not observe the bidirectional regulation of the other gene that we observed with CRISPRi. To confirm these changes are consistent at the protein levels, we performed Western blots with NAB2 or EGR3 antibodies. Neuro2a cells transfected with *Nab2* sgRNAs and CRISPRi displayed significant reduction of NAB2 protein expression, while EGR3 protein expression was upregulated compared with lacZ sgRNA controls (one-way ANOVA, NAB2: interaction $F_{(3,8)} = 27.33$; $p = 0.0001$, Tukey post-test: $^{*}p < 0.05$, $^{**}p < 0.01$; EGR3: interaction $F_{(3,8)} = 26.03$; $p < 0.001$, Tukey post-test: $^{*}p < 0.05$, $^{**}p < 0.01$; protein $n = 3$ per group; Fig. 3*C*). In cells transfected with *Egr3* sgRNA and CRISPRi, we observed reduction of EGR3 protein expression, while NAB2 protein expression was upregulated compared with lacZ sgRNA controls (one-way ANOVA, NAB2: interaction $F_{(3,8)} = 27.33$; $p = 0.0001$, Tukey post-test: $^{*}p < 0.05$, $^{**}p < 0.01$; EGR3: interaction $F_{(3,8)} = 26.03$; $p < 0.001$, Tukey post-test: $^{*}p < 0.05$, $^{**}p < 0.01$; protein $n = 3$ per group; Fig. 3*C*). Contrarily, cells transfected with *Nab2* sgRNA and CRISPRa showed significant upregulation of NAB2 protein expression, and reduced EGR3 protein expression compared with lacZ sgRNA controls (one-way ANOVA, NAB2: interaction $F_{(3,8)} = 6.264$; $p = 0.05$, Tukey post-test: $^{*}p < 0.05$; EGR3: interaction $F_{(3,8)} = 154.6$; $p < 0.0001$, Tukey post-test: $^{**}p < 0.01$, $^{****}p < 0.0001$; protein $n = 3$ per group; Fig. 3*C*). In cells transfected with CRISPRa targeted by *Egr3* sgRNA, we saw an induction of EGR3 protein expression while NAB2 protein expression did not change compared with lacz sgRNA controls (one-way ANOVA, NAB2: interaction $F_{(3,8)} = 6.264$; $p < 0.05$, Tukey post-test: $^{*}p < 0.05$; EGR3: interaction $F_{(3,8)} = 154.6$; $p < 0.0001$, Tukey post-test: $^{**}p < 0.01$, $^{****}p < 0.0001$; protein $n = 3$ per group; Fig. 3*C*). Notably, we observed that transfection with *Nab2*-363 gRNA was able to induce the changes in *Nab2* and *Egr3* in both the CRISPRi and CRISPRa systems compared with *Nab2*-729, suggesting that targeting closer to the ATG site provides improved efficiency for targeting of *Nab2*. We focused on this gRNA target in subsequent validation of CRISPRi/CRISPRa.

To validate the CRISPRi and CRISPRa specificity, we performed Cut&Run experiments (Skene and Henikoff, 2017) with anti-HA to target the HA-tag on the CRISPRi/CRISPRa vectors, as well as antibodies against hallmark activation and repressive histone methylation and acetylation modifications H3K4me3 and H3K27ac (Wysocka et al., 2006; Heintzman et al., 2007, 2009; Wang et al., 2008; Creyghton et al., 2010; Rudolph et al., 2013). In Neuro2a cells transfected with *Nab2* sgRNA and CRISPRi system, we saw an increase in the enrichment of CRISPRi complex on *Nab2* promoter compared with lacZ sgRNA controls (one-way ANOVA, interaction $F_{(2,22)} = 14.78$; $p < 0.0001$, Tukey post-test: $^{**}p < 0.01$, $^{***}p < 0.001$; Cut&Run chromatin $n = 7$-9 per group; Fig. 3*D*). In samples with the *Egr3* sgRNA CRISPRi system, we observed an increase in the enrichment of CRISPRi complex on the *Egr3* promoter compared with lacZ sgRNA controls (one-way ANOVA, interaction $F_{(2,22)} = 4.200$; $p = 0.0273$, Tukey post-test: $^{*}p < 0.05$; Cut&Run chromatin $n = 7$-9 per group; Fig. 3*D*). Interestingly, we observed no significant change in the enrichment of H3K4me3 on the *Nab2* promoter with the *Nab2* sgRNA CRISPRi system, but we did observe a decrease of H3k4me3 enrichment on the *Egr3* promoter with the *Egr3* sgRNA CRISPRi system (one-way ANOVA, *Nab2*: interaction $F_{(2,23)} = 3.343$; $p = 0.0532$, Tukey post-test: $^{*}p < 0.05$. *Egr3*: interaction $F_{(2,24)} = 19.20$; $p < 0.0001$, Tukey post-test: $^{***}p < 0.001$, $^{****}p < 0.0001$; Cut&Run chromatin $n = 8$ or 9 per group; Fig. 3*D*). Consistent with the changes in the mRNA and protein levels of *Nab2* and *Egr3* when targeted with CRISPRi, H3K27ac enrichment on *Nab2* and *Egr3* promoters was decreased *Nab2* sgRNA CRISPRi and *Egr3* sgRNA CRISPRi targeting, respectively (one-way ANOVA, *Nab2*: interaction $F_{(2,22)} = 17.41$; $p < 0.0001$, Tukey post-test: $^{***}p < 0.001$, $^{****}p < 0.0001$; *Egr3*: interaction $F_{(2,24)} = 63.33$; $p < 0.0001$, Tukey post-test: $^{****}p < 0.0001$; Cut&Run chromatin $n = 7$-9 per group; Fig. 3*D*). These results demonstrate the target specificity of CRISPRi system and suggest that deacetylation at the H3K27 mark may drive the mRNA and protein level changes of target genes using the CRISPRi system. Consistent with our findings in CRISPRi Cut&Run experiments, the enrichment of CRISPRa complex on the *Nab2* and *Egr3* promoters was increased in cells transfected with CRISPRa targeted with *Nab2* and *Egr3* sgRNAs, respectively, compared with lacZ sgRNA controls (one-way ANOVA, *Nab2*: interaction $F_{(2,24)} = 9.147$; $p < 0.01$, Tukey post-test: $^{**}p < 0.01$;

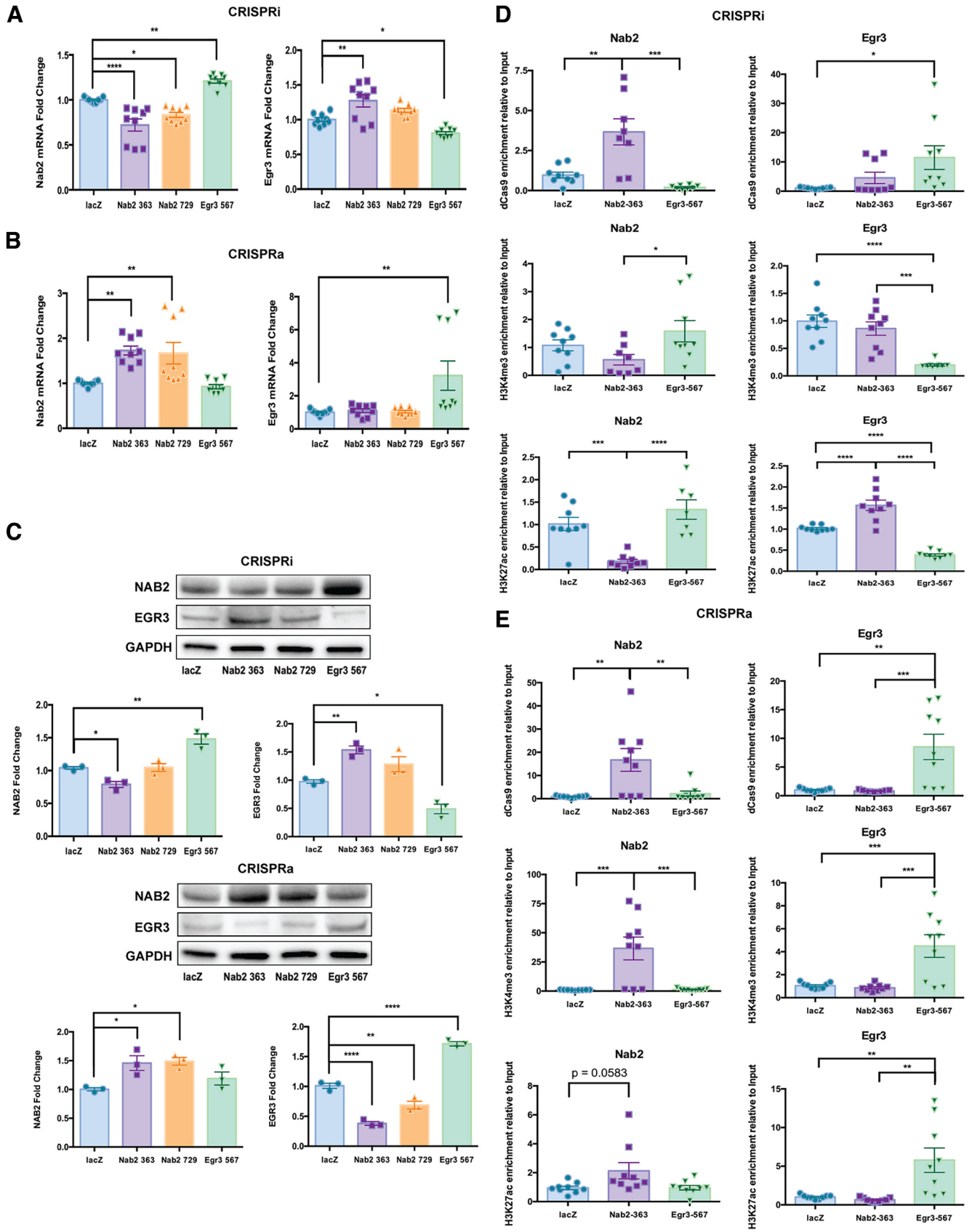

Figure 3. CRISPRi and CRISPRa manipulation of *Nab2* and *Egr3* transcription. ***A***, qRT-PCR shows *Nab2*-targeted CRISPRi repressed *Nab2* mRNA while inducing *Egr3* mRNA expression, and *Egr3*-targeted CRISPRi repressed *Egr3* mRNA while inducing *Nab2* mRNA expression in Neuro2a cells ($n = 9$ per condition). ***B***, Conversely, *Nab2*-targeted CRISPRa activates *Nab2* mRNA expression, and *Egr3*-targeted CRISPRa activates *Egr3* mRNA expression in Neuro2a cells ($n = 9$ per condition). ***C***, Western blots using Neuro2a cells transfected with *Nab2*-targeted CRISPRi show downregulation of NAB2 and upregulation of EGR3, while cells transfected with *Nab2*-targeted CRISPRa show upregulation of NAB2 and downregulation of EGR3. Consistently, Neuro2a cells transfected with *Egr3*-targeted CRISPRi samples show downregulation of EGR3 and upregulation of NAB2, while cells transfected with *Egr3*-targeted CRISPRa show upregulation of EGR3 but

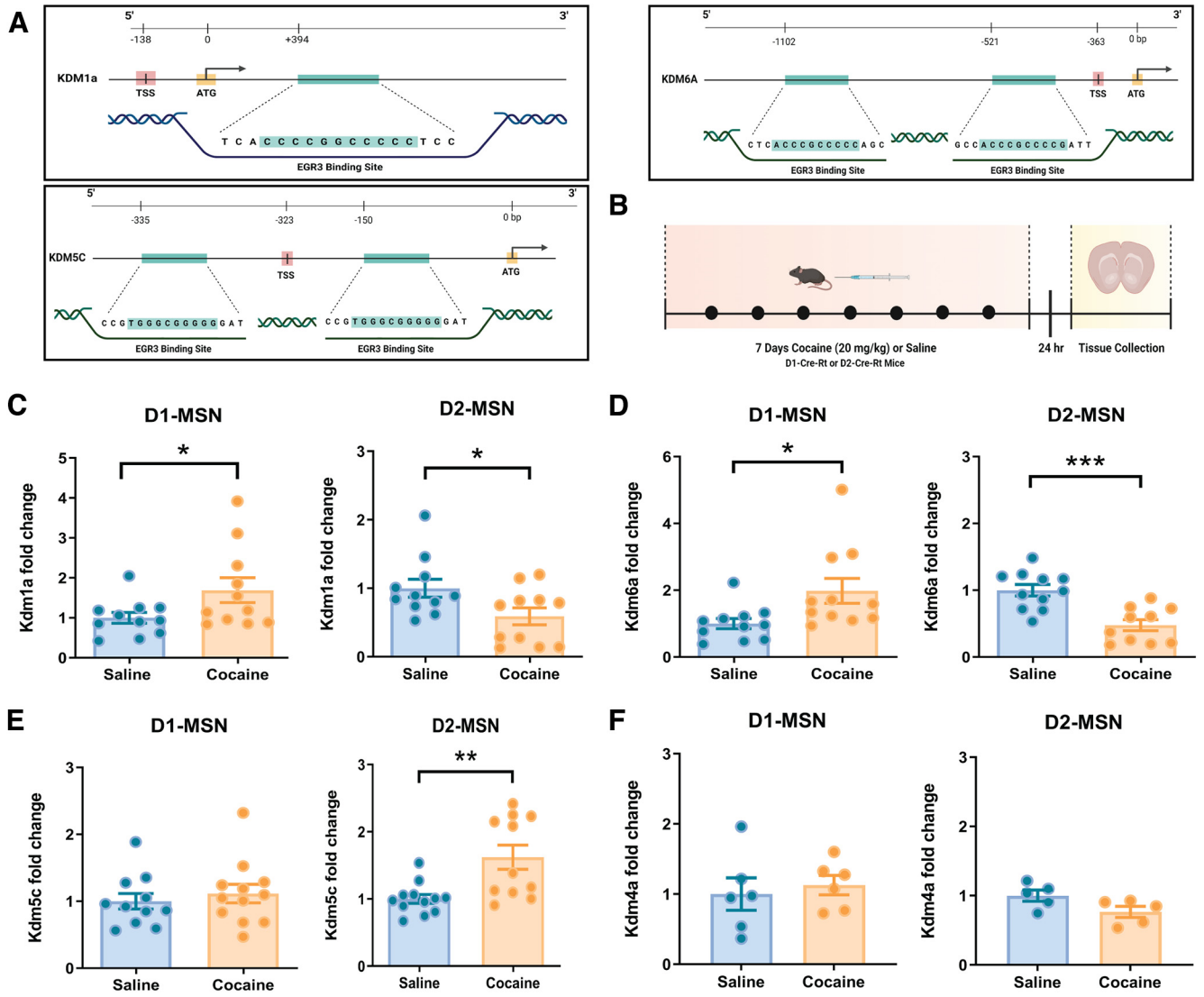

Figure 4. Kdms display bidirectional expression patterns in D1-MSNs and D2-MSNs after repeated cocaine exposure. ***A***, *Kdm1a*, *Kdm6a*, and *Kdm5c* have GC-rich EGR3 putative binding sites in the promoter and near the transcription start site. ***B***, Male *D1-Cre-RT* and *D2-Cre-RT* mice received seven daily injections of cocaine (20 mg/kg). Tissue punches were collected 24 h after last injection. ***C***, qRT-PCR shows increased *Kdm1a* mRNA in D1-MSNs, while it decreased in D2-MSNs (D1-MSNs saline $n = 11$, cocaine $n = 11$; D2-MSNs saline $n = 11$, cocaine $n = 11$). ***D***, Consistently, qRT-PCR shows increased Kdm6a mRNA levels in D1-MSNs, while it decreased in D2-MSNs (D1-MSNs saline $n = 11$, cocaine $n = 11$; D2-MSNs saline $n = 11$, cocaine $n = 10$). ***E***, qRT-PCR shows decreased *Kdm5c* mRNA levels in D2-MSNs, while it did not change in D1-MSNs (D1-MSNs saline $n = 11$, cocaine $n = 12$; D2-MSNs saline $n = 12$, cocaine $n = 11$). ***F***, No changes were observed in *Kdm4a* mRNA levels in either D1- or D2-MSNs (D1-MSNs saline $n = 6$, cocaine $n = 6$; D2-MSNs saline $n = 5$, cocaine $n = 5$). Error bar indicates mean ± SEM. $^{*}p < 0.05$. $^{**}p < 0.01$. $^{***}p < 0.001$.

Egr3: interaction $F_{(2,24)} = 11.71$; $p < 0.001$, Tukey post-test: $^{**}p < 0.01$, $^{***}p < 0.001$; Cut&Run chromatin $n = 9$ per group; Fig. 3*E*). Enrichment of H3K4me3 on the *Nab2* and *Egr3* promoters were significantly increased with *Nab2* sgRNA CRISPRa and *Egr3* sgRNA CRISPRa targeting, respectively, compared with lacZ sgRNA controls (one-way ANOVA, *Nab2*: interaction $F_{(2,24)} = 13.14$; $p = 0.0001$, Tukey post-test: $^{***}p < 0.001$. *Egr3*: interaction $F_{(2,24)} = 12.78$; $p < 0.001$, Tukey post-test: $^{***}p < 0.001$; Cut&Run chromatin $n = 9$ per group; Fig. 3*E*). Enrichment of H3K27ac on the *Nab2* promoter was trending toward a significant increase compared with lacZ control with *Nab2* sgRNA CRISPRa targeting, and H3K27ac enrichment on the *Egr3* promoter was significantly increased relative to lacZ control with *Egr3* sgRNA CRISPRa targeting (one-way ANOVA, *Nab2*: interaction $F_{(2,24)} = 3.885$; $p = 0.0345$, Tukey post-test: not significant; *Egr3*: interaction $F_{(2,24)} = 9.756$; $p < 0.001$, Tukey post-test: $^{**}p < 0.01$; Cut&Run chromatin $n = 9$ per group; Fig. 3*E*). These results reveal the target specificity of the CRISPRa system, and suggest that H3K27 acetylation and H3K4 trimethylation may drive the mRNA and protein level changes of target genes using CRISPRa.

Histone lysine demethylases display bidirectional induction in NAc D1-MSNs and D2-MSNs after repeated cocaine

Since EGR3 has predicted binding sites within *Kdm1a*, *Kdm6a*, and *Kdm5c* genes (http://gene-regulation.com/pub/programs/alibaba2/)

←

did not change NAB2 levels ($n = 3$ per condition). ***D***, Cut&Run of Neuro2a cells transfected with CRISPRi show HA-tag enrichment on the promoters of respective genes targeted by sgRNAs. Transcriptional activation marks, H3K4me3 and H3K27ac, display reduced enrichment on the promoters of respective genes targeted by sgRNAs compared with lacZ controls ($n = 7$-9 per condition). ***E***, Cut&Run of Neuro2a cells transfected with CRISPRa show HA-tag, H3K4me3, and H3K27ac enrichment on the promoters of respective genes targeted by sgRNAs compared with lacZ controls ($n = 9$ per condition). Error bar indicates mean ± SEM. $^{*}p < 0.05$. $^{**}p < 0.01$. $^{***}p < 0.001$. $^{****}p < 0.0001$.

(Fig. 4*A*), we next investigated NAc D1 and D2-MSN cell subtype ribosome-associated mRNA of *Kdm1a*, *Kdm5c*, and *kdm6a*, together with *Kdm4a* which does not have a putative binding site with EGR3, after seven daily injections of cocaine (20 mg/kg) followed by a 24 h abstinent period in *D1-Cre-RT* and *D2-Cre-RT* mice (Fig. 4*B*). *Kdm1a* mRNA was increased in NAc D1-MSNs, while decreased in D2-MSNs of cocaine exposed mice compared with saline controls (Student's *t* test, $^{*}p < 0.05$; mRNA sample $n = 11$ per group, $t_{(20)} = 2.279$, $p < 0.05$; mRNA sample $n = 11$ per group, $t_{(20)} = 2.279$, $p < 0.05$; Fig. 4*C*). Similarly, *Kdm6a* mRNA was increased in D1-MSNs, while decreased in D2-MSNs in this condition (Student's *t* test, $^{*}p < 0.05$, $^{***}p < 0.001$; mRNA sample $n = 11$ per group, $t_{(20)} = 2.436$, $p < 0.05$; mRNA sample $n = 10$ or 11 per group, $t_{(19)} = 4.364$, $p < 0.001$; Fig. 4*D*). In contrast, *Kdm5c* mRNA was increased in D2-MSNs, while D1-MSNs did not show a significant change with repeated exposure to cocaine (Student's *t* test, $^{**}p < 0.01$; mRNA sample $n = 11$ or 12 per group, $t_{(21)} = 0.6308$, $p = 0.5350$; mRNA sample $n = 11$ or 12 per group, $t_{(21)} = 3.341$, $p < 0.01$; Fig. 4*E*). Notably, we did not observe a change in *Kdm4a*, which lacks a putative EGR3 binding site, in either D1-MSNs or D2-MSNs after repeated exposure to cocaine (Student's *t* test; mRNA sample $n = 6$ per group, $t_{(10)} = 0.4764$, $p = 0.6440$; mRNA sample $n = 5$ per group, $t_{(8)} = 2.060$, $p = 0.0733$; Fig. 4*F*).

Light-inducible Opto-CRISPR-KDM1A and Opto-CRISPR-p300 system allows spatiotemporally precise perturbation of *Nab2* and *Egr3* expression

Given bidirectional induction of some *Kdm*s in NAc cell subtypes (Fig. 4*C–E*) and the enrichment of KDM1A on both *Egr3* and *Nab2* promoters in total NAc (Fig. 1*D*) after repeated cocaine, we next explored whether targeting KDM1A to *Egr3* and *Nab2* promoters can alter these transcripts in Neuro2A cells similar to cocaine exposure in NAc MSNs. To do this, we used a Cre- and light-inducible CRISPR-KDM1A system (Opto-CRISPR-KDM1A) which utilizes the blue light-inducible CRY2-CIB heterodimerizing system (Kennedy et al., 2010; Hughes et al., 2012; Konermann et al., 2013; Nihongaki et al., 2015; Polstein and Gersbach, 2015; Taslimi et al., 2016). By fusing the N-terminal fragment of CIB1 with dCas9 (DIO-dCas9-HA-CIBN), and truncated CRY2 with KDM1A (DIO-CRY2-FLAG-KDM1A), we developed a system to deliver KDM1A-induced histone demethylation with spatiotemporal precision and Cre-dependent specificity (Fig. 5*A*). First, we transfected these vectors together with lacZ sgRNA in Neuro2a cells to confirm that these vectors express only in Cre-positive cells. Forty-eight hours after transfection, we immunostained cells for DAPI, GFP, HA-tag, and FLAG-tag. We observed GFP, HA-tag, and FLAG-tag signals only in Cre-positive cells, while Cre-negative cells lacked these signals (Fig. 5*B*). To address the possibility of functional promiscuity for unbound KDM1A, we compared *Nab2* and *Egr3* mRNA expression in Neuro2a cells transfected only with DIO-CRY2-FLAG-KDM1A and Cre vectors to cells transfected with Opto-CRISPR-KDM1A system targeted by lacZ sgRNA. In cells transfected only with DIO-CRY2-FLAG KDM1A and Cre vectors, we did not observe significant changes in *Nab2* or *Egr3* mRNA levels compared with cells transfected with Opto-CRISPR-KDM1A targeted by lacZ sgRNA after 2 h of 1 mW blue light stimulation (Student's *t* test; mRNA sample $n = 3$ per group, $t_{(4)} = 0.2908$, $p = 0.7857$; mRNA sample $n = 3$ per group, $t_{(4)} = 0.8796$, $p = 0.4287$; Fig. 5*C*). To investigate whether blue light stimulation itself may alter the expression of our target genes, we compared the mRNA expression of *Nab2* and *Egr3* in Neuro2a cells transfected with Opto-CRISPR-KDM1A targeted by lacZ sgRNA in no light condition or 2 h of 1 mW blue light stimulation. Between these two conditions, we did not observe significant changes in *Nab2* or *Egr3* mRNA levels (Student's *t* test; mRNA sample $n = 3$ per group, $t_{(4)} = 1.183$, $p = 0.3023$; mRNA sample $n = 3$ per group, $t_{(4)} = 2.126$, $p = 0.1006$; Fig. 5*D*). To avoid potential blue light-induced gene expression alterations from phototoxicity, we changed the culture media to Photostable NEUMO media at least 3 h before the start of light stimulations in all of the experiments performed in this study (Duke et al., 2019).

We next used the Opto-CRISPR-KDM1A with *Nab2* sgRNA or *Egr3* sgRNA to determine whether recruiting KDM1A to these promoters can reduce or enhance transcription since KDM1A demethylates both positive and repressive histone marks. Using Opto-CRISPR-KDM1A with *Nab2* sgRNA targeting, we observed a reduction in *Nab2* mRNA compared with lacZ controls after 2 h of 1 mW blue light stimulation (one-way ANOVA, *Nab2*: interaction $F_{(3,32)} = 145.8$; $p = 0.0001$, Tukey post-test: $^{**}p < 0.01$, $^{****}p < 0.0001$; mRNA $n = 9$ per group; Fig. 6*A*). In Neuro2a cells transfected with *Egr3* sgRNA and Opto-CRISPR-KDM1A, we also observed reduction of *Egr3* mRNA compared with lacZ controls after 2 h of 1 mW blue light stimulation (one-way ANOVA, *Egr3*: interaction $F_{(3,32)} = 84.44$; $p = 0.0001$, Tukey post-test: $^{****}p < 0.0001$; mRNA $n = 9$ per group; Fig. 6*A*). Consistent with our findings with CRISPRi, *Nab2* mRNA was upregulated compared with lacZ controls with Opto-CRISPR-KDM1A and *Egr3* sgRNA targeting (one-way ANOVA, *Nab2*: interaction $F_{(3,32)} = 145.8$; $p = 0.0001$, Tukey post-test: $^{**}p < 0.01$, $^{****}p < 0.0001$; mRNA $n = 9$ per group; Fig. 6*A*). These results suggest that Opto-CRISPR-KDM1A interacts with nucleosome remodeling and histone deacetylase (NuRD) complex to cause demethylation at H3K4 methyl sites, resulting in transcriptional repression (Wang et al., 2009; Basta and Rauchman, 2015). Consistent observations were made at the protein level of NAB2 and EGR3 via Western blots. Two hours of 1 mW blue light stimulation in Neuro2a cells transfected with Opto-CRISPR-KDM1A targeted by Nab2 sgRNA reduced NAB2 protein expression and induced EGR3 protein expression compared with lacZ controls (one-way ANOVA, NAB2: interaction $F_{(3,8)} = 7.602$; $p = 0.01$, Tukey post-test: $^{*}p < 0.05$; EGR3: interaction $F_{(3,8)} = 47.89$; $p < 0.0001$, Tukey post-test: $^{**}p < 0.01$; Protein $n = 3$ per group; Fig. 6*B*). In cells transfected with Opto-CRISPR-KDM1A targeted by *Egr3* sgRNA, 2 h of 1 mW blue light stimulation reduced EGR3 protein expression compared with lacZ controls (one-way ANOVA, EGR3: interaction $F_{(3,8)} = 47.89$; $p < 0.0001$, Tukey post-test: $^{**}p < 0.01$; Protein $n = 3$ per group; Fig. 6*B*). To validate the specificity of Opto-CRISPR-KDM1A in our findings, we performed Cut&Run experiments with anti-HA to target the HA-tag on the dCas9-CIBN portion of the vectors, as well as antibodies against hallmark activation and repressive histone methylation and acetylation modifications H3K4me3 and H3K27ac (Shi et al., 2004; Wysocka et al., 2006; Robison and Nestler, 2011; Ferrari et al., 2014; Nestler, 2014). In Neuro2a cells transfected with Opto-CRISPR-KDM1A with *Nab2* sgRNA, we observed an increase in the enrichment of Opto-CRISPR-KDM1A complex on the *Nab2* promoter compared with lacZ sgRNA controls (one-way ANOVA, *Nab2*: interaction $F_{(2,24)} = 24.93$; $p < 0.0001$, Tukey post-test: $^{****}p < 0.0001$; Cut&Run chromatin $n = 9$ per group; Fig. 6*C*). In cells transfected with Opto-CRISPR-KDM1A with *Egr3* sgRNA, we observed an

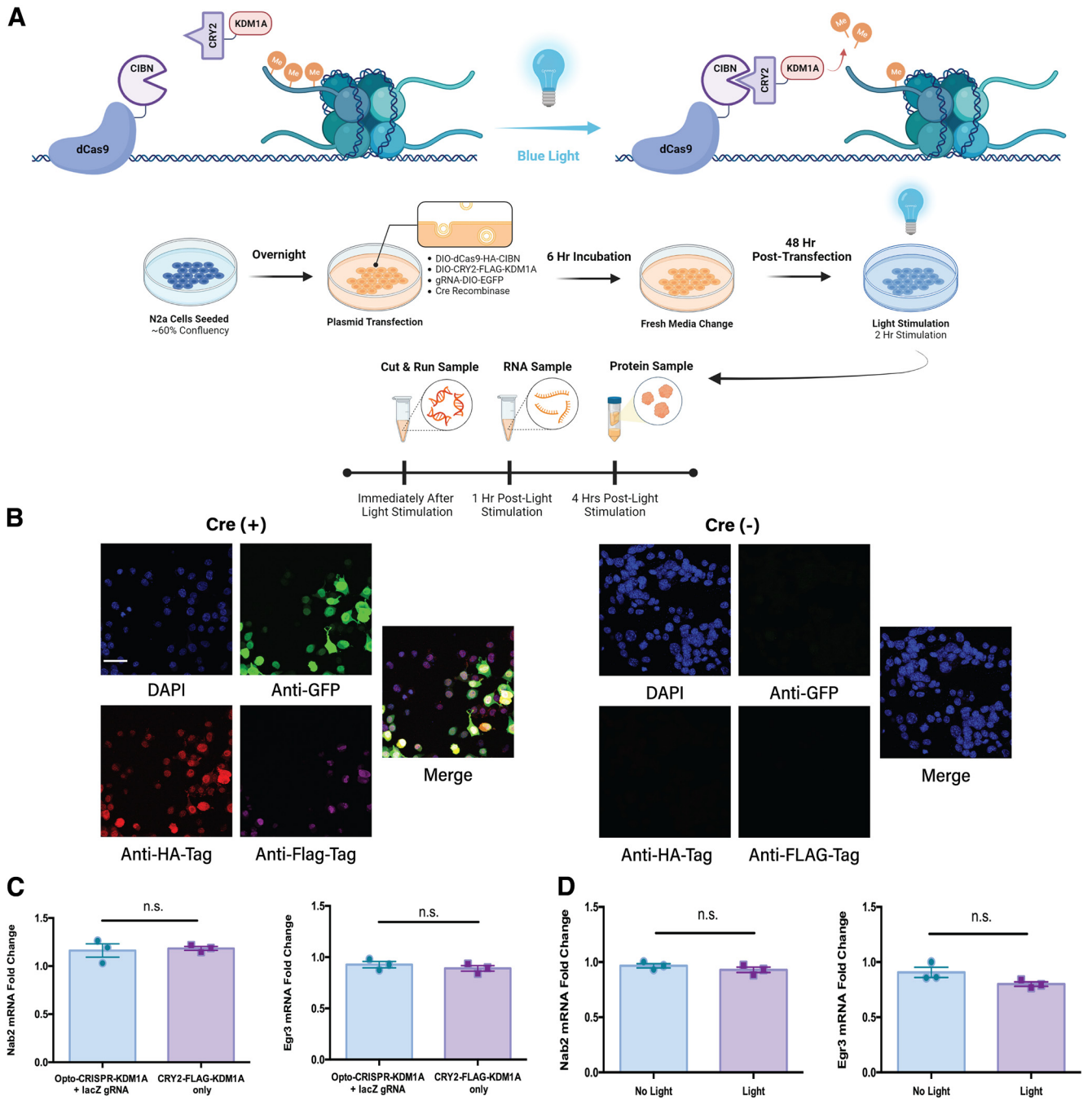

Figure 5. Development of a Cre- and light-inducible Opto-CRISPR-KDM1A system. ***A***, Illustration of light-inducible dCas9 and KDM1A fusion complex using CIBN and CRY2 heterodimers. Neuro2a cells received 2 h of 1 mW blue light stimulation. ***B***, Immunocytochemistry of Neuro2a cells transfected with Opto-CRISPR-KDM1A display a Cre-inducible expression as observed by GFP (green), HA-Tag (red), and Flag-Tag (magenta) expression. Blue represents DAPI signal. Scale bar, 50 μm. ***C***, qRT-PCR demonstrates cells transfected only with DIO-CRY2-FLAG-KDM1A, and Cre vectors do not show significant changes in *Nab2* or *Egr3* mRNA levels compared with cells transfected with complete Opto-CRISPR-KDM1A targeted by lacZ sgRNA after 2 h of blue light stimulation ($n = 3$ per condition). ***D***, qRT-PCR demonstrates that Neuro2a cells transfected with Opto-CRISPR-KDM1A with lacZ sgRNA in no light condition and 2 h of 1 mW blue light stimulation do not display significant differences in *Nab2* and *Egr3* mRNA levels ($n = 3$ per condition). Error bar indicates mean ± SEM.

increase in the enrichment of Opto-CRISPR-KDM1A complex on *Egr3* promoter compared with lacZ sgRNA controls (one-way ANOVA, *Egr3*: interaction $F_{(2,24)} = 16.01$; $p < 0.0001$, Tukey post-test: $^{***}p < 0.001$; Cut&Run chromatin $n = 9$ per group; Fig. 6*C*). Consistent with the changes in the mRNA and protein levels of *Nab2* and *Egr3* when targeted with Opto-CRISPR-KDM1A and their respective sgRNAs, H3K27ac and H3K4me3 enrichment on *Nab2* promoter was decreased in *Nab2* sgRNA Opto-CRISPR-KDM1A system and H3K27ac and H3K4me3 enrichment on *Egr3* promoter was decreased in the *Egr3* sgRNA Opto-CRISPR-KDM1A system (one-way ANOVA, H3K27ac *Nab2*: interaction $F_{(2,24)} = 32.07$; $p < 0.0001$, Tukey post-test: $^{**}p < 0.01$, $^{***}p < 0.001$, $^{****}p < 0.0001$; H3K27ac *Egr3*: interaction $F_{(2,24)} = 7.654$; $p < 0.01$, Tukey post-test: $^{*}p < 0.05$, $^{**}p < 0.01$; H3K4me3 *Nab2*: interaction $F_{(2,23)} = 6.646$; $p < 0.01$, Tukey post-test: $^{**}p < 0.01$; H3K4me3 *Egr3*: interaction $F_{(2,24)} = 5.188$; $p < 0.05$, Tukey post-test: $^{*}p < 0.05$; Cut&Run chromatin $n = 8$ or 9 per group; Fig. 6*C*). These results demonstrate the target specificity of Opto-CRISPR-KDM1A system. Furthermore, these results show that KDM1A targeting with *Nab2* or *Egr3* sgRNAs causes a transcriptionally

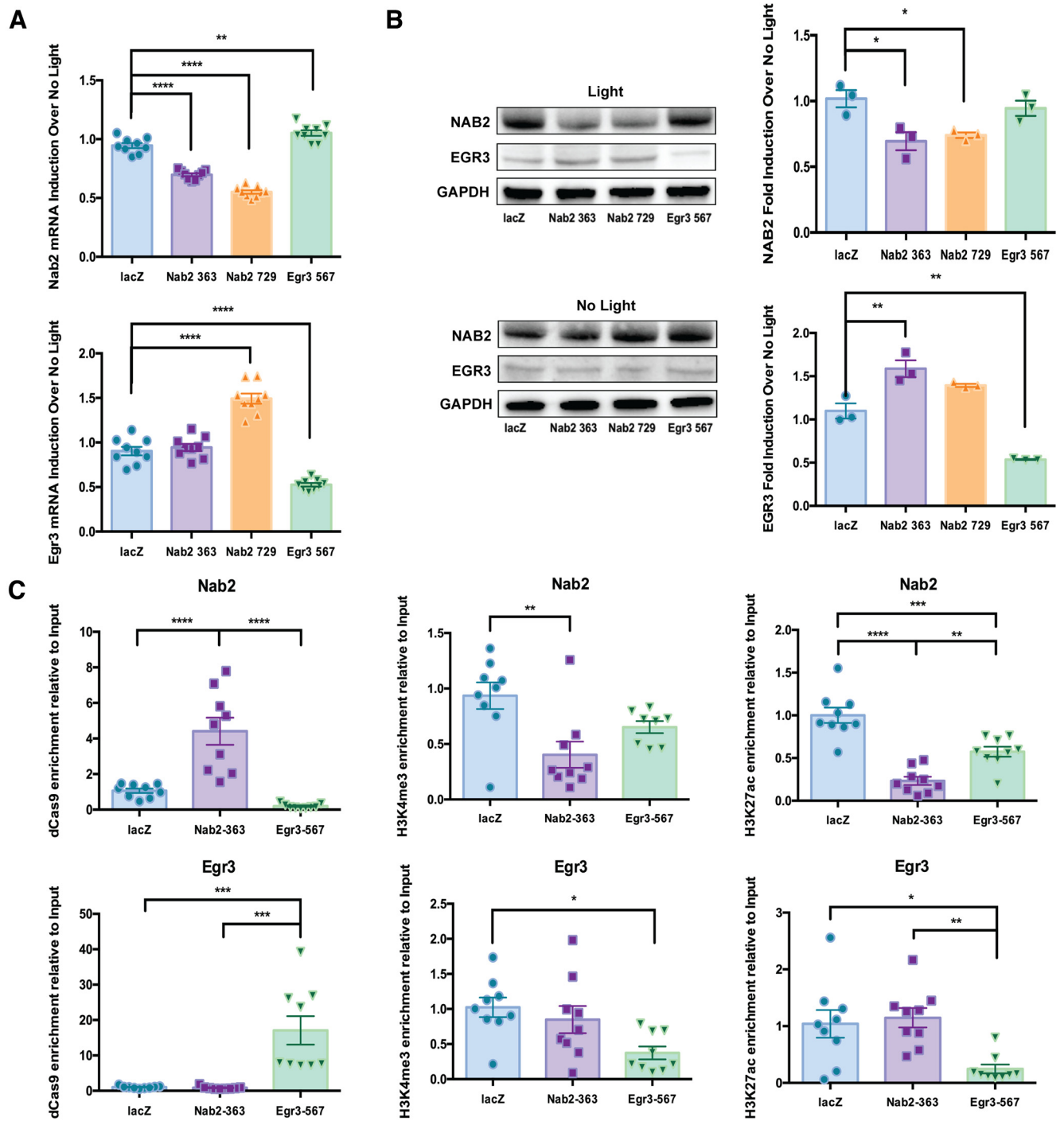

Figure 6. Opto-CRISPR-KDM1A mediated inhibition of *Nab2* and *Egr3* transcription. ***A***, qRT-PCR demonstrates that 2 h of blue light stimulation downregulated *Nab2* mRNA while inducing *Egr3* mRNA expression in cells transfected with *Nab2*-targeted Opto-CRISPR-KDM1A. Conversely, 2 h of blue light stimulation induced *Nab2* mRNA while downregulating *Egr3* mRNA expression in cells transfected with Opto-CRISPR-KDM1A and *Egr3* sgRNA ($n = 9$ per condition). ***B***, Western blots represent 2 h of blue light stimulation downregulated NAB2 levels, while upregulating EGR3 levels in cells transfected Opto-CRISPR-KDM1A and *Nab2* sgRNA. EGR3 levels were downregulated, while NAB2 levels were unchanged in cells transfected with Opto-CRISPR-KDM1A and *Egr3* sgRNA ($n = 3$ per condition). ***C***, Cut&Run on blue light stimulated Neuro2a cells transfected with Opto-CRISPR-KDM1A shows enrichment of Opto-CRISPR-KDM1A complex on the promoters of respective genes targeted by sgRNAs compared with lacZ sgRNA controls. Transcriptional activation marks, H3K4me3 and H3K27ac, have reduced enrichment on the promoters of respective genes targeted by sgRNAs compared with lacZ sgRNA controls ($n = 9$ per condition). Error bar indicates mean ± SEM. *$p < 0.05$. **$p < 0.01$. ***$p < 0.001$. ****$p < 0.0001$.

repressive H3K4 demethylase function for KDM1A rather than a transcription inducive H3K9 demethylase function (Shi et al., 2004; Metzger et al., 2005).

Since Opto-CRISPR-KDM1A acts to repress transcription when targeted to *Egr3* and *Nab2*, Opto-CRISPRi, we then wanted to use an Opto-CRISPRa approach. To do this, we developed a new opto-CRISPR-p300 vector in which KDM1A portion of DIO-CRY2-FLAG-KDM1A vector was replaced by the truncated p300 functional core (DIO-CRY2-FLAG-p300Core) to induce histone acetylation at the H3K27 mark (Fig. 7*A*) (Delvecchio et al., 2013; Hilton et al., 2015). We first performed immunohistochemistry in Neuro2a cells transfected with Opto-CRISPR-p300, lacZ sgRNA, and Cre to demonstrate that the vectors express only within Cre-positive cells (Fig. 7*B*). To address the possibility

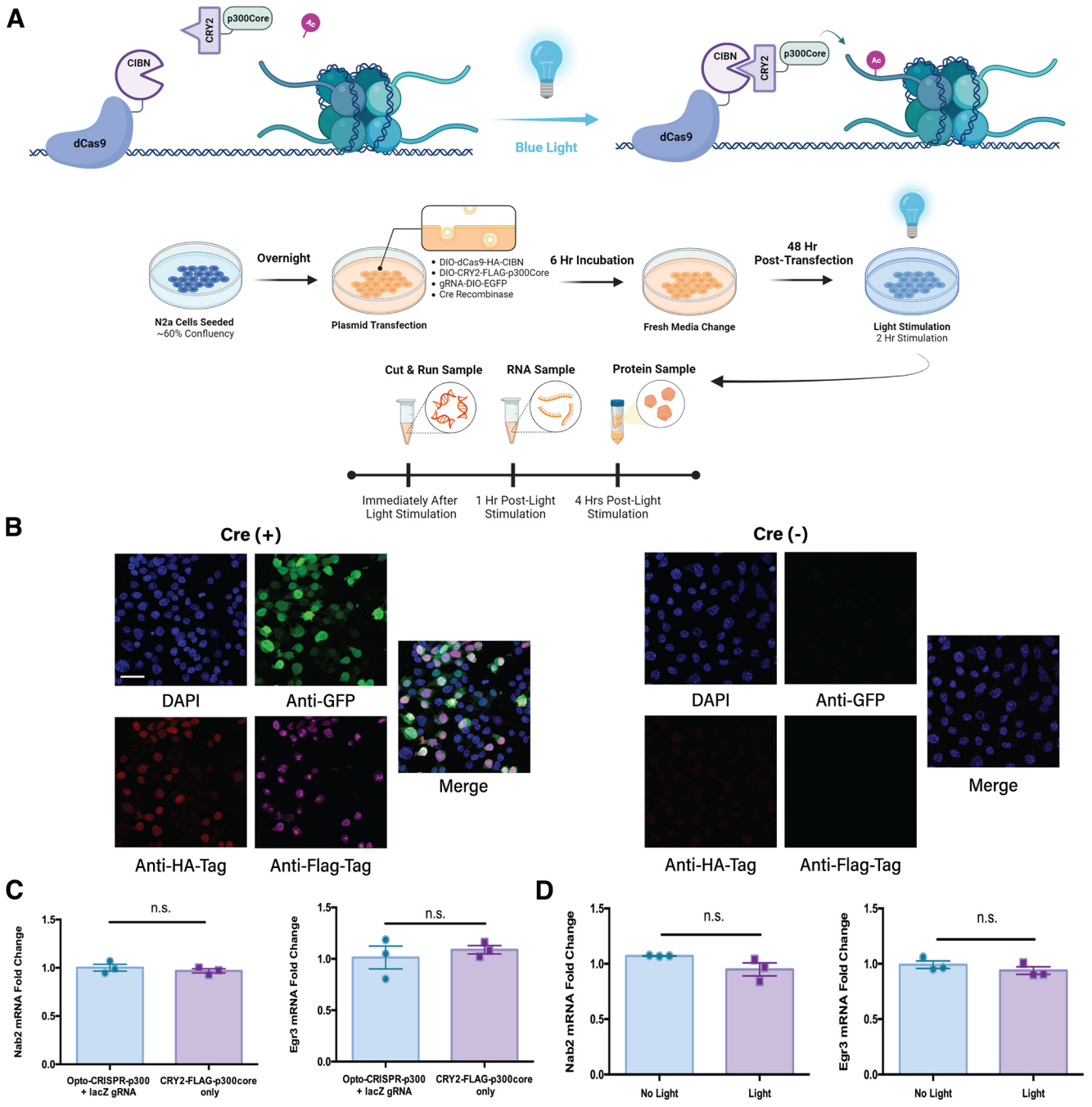

Figure 7. Development of a Cre- and light-inducible Opto-CRISPR-p300 system. ***A***, Illustration of light-inducible dCas9 and p300 fusion complex using CIBN and CRY2 heterodimers. Neuro2a cells received 2 h of 1 mW blue light stimulation. ***B***, Immunocytochemistry of Neuro2a cells transfected with Opto-CRISPR-p300 system demonstrates a Cre-inducible expression as observed by GFP (green), HA-Tag (red), and Flag-Tag (magenta) expression. Blue represents DAPI signal. Scale bar, 50 μm. ***C***, qRT-PCR demonstrates that the expression of DIO-CRY2-FLAG-p300core alone does not induce changes in *Nab2* or *Egr3* mRNA levels compared with cells transfected with Opto-CRISPR-p300 targeted by lacZ sgRNA after 2 h of blue light stimulation ($n = 3$ per condition). ***D***, qRT-PCR demonstrates Neuro2a cells transfected with Opto-CRISPR-p300 targeted by lacZ sgRNA in no light condition and 2 h of 1 mW blue light stimulation do not display significant differences in *Nab2* and *Egr3* mRNA levels ($n = 3$ per condition). Error bar indicates mean ± SEM.

of functional promiscuity for unbound p300core, we compared the mRNA expression of *Nab2* and *Egr3* in Neuro2a cells transfected only with DIO-CRY2-FLAG-p300core and Cre vectors to cells transfected with Opto-CRISPR-p300 and lacZ sgRNA. In cells transfected only with DIO-CRY2-FLAG-p300core, we did not observe significant changes in *Nab2* or *Egr3* mRNA levels compared with cells transfected with Opto-CRISPR-p300 and lacZ sgRNA after 2 h of 1 mW blue light stimulation (Student's *t* test; mRNA sample $n = 3$ per group, $t_{(4)} = 0.7803$, $p = 0.4788$; mRNA sample $n = 3$ per group, $t_{(4)} = 0.6398$, $p = 0.5571$; Fig. 7*C*). To determine whether blue light stimulation itself may alter the expression of our target genes, we compared the mRNA expression of *Nab2* and *Egr3* in Neuro2a cells transfected with Opto-CRISPR-p300 with lacZ sgRNA in no light condition and 2 h of 1 mW blue light stimulation. Between these two conditions, we did not observe significant changes in *Nab2* or *Egr3* mRNA levels (Student's *t* test; mRNA sample $n = 3$ per group, $t_{(4)} = 2.072$, $p = 0.1070$; mRNA sample $n = 3$ per group, $t_{(4)} = 1.098$, $p = 0.3340$; Fig. 7*D*).

We then transfected Opto-CRISPR-p300 with *Nab2* sgRNA or *Egr3* sgRNA into Neuro2a cells. After 2 h of 1 mW blue light stimulation, *Nab2* mRNA and *Egr3* mRNA were significantly increased compared with lacZ controls when targeting with their respective gRNAs (one-way ANOVA, *Nab2*: interaction $F_{(3,32)} = 3.872$; $p < 0.05$, Tukey post-test: $^{*}p < 0.05$. *Egr3*: interaction $F_{(3,32)} = 13.03$; $p < 0.0001$, Tukey post-test: $^{**}p < 0.01$; mRNA $n = 9$ per group; Fig. 8*A*). These results were consistent in protein expression demonstrated via Western blots, as 2 h of 1 mW blue light stimulation in Neuro2a cells transfected with Opto-CRISPR-p300 with *Nab2* sgRNA induced NAB2 protein expression. Notably, EGR3 expression was induced in these cells compared with lacZ controls, although this bidirectional regulation was not observed at the mRNA level (one-way ANOVA, NAB2: interaction $F_{(3,8)} = 5.296$; $p < 0.05$, Tukey post-test: $^{*}p < 0.05$; EGR3: interaction $F_{(3,8)} = 19.78$; $p < 0.001$, Tukey post-test: $^{*}p < 0.05$; Protein $n = 3$ per group; Fig. 8*B*). In cells transfected with Opto-CRISPR-p300 targeted by *Egr3* sgRNA, 2 h of 1 mW blue light stimulation induced EGR3 protein expression compared with lacZ controls (one-way ANOVA, EGR3: interaction $F_{(3,8)} = 19.78$; $p < 0.001$, Tukey post-test: $^{*}p < 0.05$; Protein $n = 3$ per group; Fig. 8*B*). To validate the specificity of Opto-CRISPR-p300, we performed Cut&Run experiments with anti-HA to target the HA-tag on the dCas9-CIBN as well as anti-H3K4me3 and anti-H3K27ac. In Neuro2a cells transfected with Opto-CRISPR-p300 with *Nab2* sgRNA, we saw an increase in the enrichment of Opto-CRISPR-p300 complex on the *Nab2* promoter compared with lacZ sgRNA controls (one-way ANOVA, *Nab2*: interaction $F_{(2,23)} = 35.67$; $p < 0.0001$, Tukey post-test: $^{****}p < 0.0001$; Cut&Run chromatin $n = 8$ or 9 per group; Fig. 8*C*). When using the *Egr3* sgRNA, we observed an increase in the enrichment of Opto-CRISPR-p300 complex on the *Egr3* promoter compared with lacZ sgRNA controls (one-way ANOVA, *Egr3*: interaction $F_{(2,24)} = 10.31$; $p < 0.001$, Tukey post-test: $^{**}p < 0.01$; Cut&Run chromatin $n = 9$ per group; Fig. 8*C*). Notably, H3K4me3 enrichment on the *Nab2* promoter was not significantly changed in the *Nab2* sgRNA Opto-CRISPR-p300 system, while H3K4me3 enrichment on the *Egr3* promoter was decreased with *Egr3* sgRNA and Opto-CRISPR-p300 (one-way ANOVA, *Nab2*: interaction $F_{(2,22)} = 4.291$; $p < 0.05$, Tukey post-test: $^{*}p < 0.05$. *Egr3*: interaction $F_{(2,24)} = 17.82$; $p < 0.0001$, Tukey post-test: $^{***}p < 0.001$ $^{****}p < 0.0001$; Cut&Run chromatin $n = 7$-9 per group; Fig. 8*C*). Consistent with the changes in the mRNA and protein levels of *Nab2* and *Egr3* when targeted with Opto-CRISPR-p300 and their respective sgRNAs, H3K27ac enrichment on the *Nab2* promoter was increased in *Nab2* sgRNA Opto-CRISPR-p300 system and H3K27ac enrichment on *Egr3* promoter was increased in the *Egr3* sgRNA Opto-CRISPR-p300 system (one-way ANOVA, *Nab2*: interaction $F_{(2,24)} = 8.603$; $p < 0.01$, Tukey post-test: $^{**}p < 0.01$; *Egr3*: interaction $F_{(2,23)} = 20.14$; $p < 0.0001$, Tukey post-test: $^{****}p < 0.0001$; Cut&Run chromatin $n = 9$ per group; Fig. 8*C*). These results demonstrate the target specificity of the Opto-CRISPR-p300 system. Furthermore, these results show that p300core targeting using our Opto-CRISPR-p300 system induces activation of gene expression mainly driven by acetylation of H3K27 mark.

Discussion

Our study demonstrates bidirectional regulation of *Nab2* in NAc MSN subtypes after repeated cocaine exposure. *Nab2* was reduced in D1-MSNs and enhanced in D2-MSNs. As our previous work showed that *Egr3* is reduced in D2-MSNs after repeated cocaine (Chandra et al., 2015), the current data are consistent with *Nab2* acting in concert with *Egr3* to reduce *Egr3* expression (Kumbrink et al., 2010). Not surprisingly, in D1-MSNs that display induction of *Egr3* after repeated cocaine, we observed a reduction of its cotranscriptional repressor, *Nab2*. This intricate regulation was masked in NAc bulk tissue where *Nab2* mRNA was not significantly changed with repeated cocaine. Although our previous study demonstrates a modest reduction of *Egr3* in bulk NAc tissue in this condition (Chandra et al., 2015), these findings emphasize the possibility of missing critical molecular adaptations when the observations are made at the whole tissue level (Chandra et al., 2015).

Previous studies showed that *Nab2* is induced via BDNF signaling (Chandwani et al., 2013). Furthermore, previous reports demonstrated that *Egr3* is regulated via BDNF signaling (Roberts et al., 2006; Kim et al., 2012). BDNF may act preferentially in D2-MSNs through higher expression of BDNF and tyrosine receptor kinase B (TrkB) receptors, which may induce *Egr3* and *Nab2* (Lobo et al., 2010). In this study, we show that KDM1A enrichment on the promoters of *Nab2* and *Egr3* is elevated in the NAc after repeated exposure to cocaine (Fig. 1*D*). Furthermore, *Kdm1a* expression was induced in D1-MSNs, and the expression was reduced in D2-MSNs (Fig. 4*C*). We speculate that the increased levels of *Kdm1a* may further repress *Nab2* transcription in D1-MSNs, and the decreased levels of *Kdm1a* in D2-MSNs may contribute to *Egr3* and *Nab2* transcriptions to initially stay elevated. This may drive a negative feedback loop in which *Egr3* self-regulates its own transcription via induction of its corepressor *Nab2* in D2-MSNs. In contrast, the *Egr3* increase in D1-MSNs may occur through its positive feedback loop by which *Egr3* binds to its own promoter to enhance *Egr3* transcription (Kumbrink et al., 2010). Based on our previous study (Chandra et al., 2015) and the current study, we model these speculative regulations of Egr3 and Nab2 in MSN subtypes after repeated cocaine exposure (Fig. 9). It is also plausible that D1 and D2 receptor signaling contributes to this cocaine-driven bidirectional regulation of *Nab2* and *Egr3* in MSN subtypes through activation of upstream CREB regulator. D1 receptor signaling enhances cAMP-PKA-CREB signaling cascades (Carlezon et al., 2005; Surmeier et al., 2007; Suehiro et al., 2010), while Gi-coupled D2 receptor signaling blunts cAMP-PKA-CREB signaling cascades (Carlezon et al., 2005; Surmeier et al., 2007; Suehiro et al., 2010).

Consistent with the cocaine driven bidirectional regulation of *Nab2* and *Egr3*, we observed an increase in *Egr3* or *Nab2* when *Nab2* or *Egr3*, respectively, was silenced using CRISPRi in Neuro2a cells. Similarly, *Egr3* or *Nab2* was induced with CRISPRa activation of the other molecule. These bidirectional regulations closely mimicked cocaine driven regulation of *Nab2* and *Egr3* observed in MSN subtypes. Our previous work demonstrated D2-MSN-specific downregulation of *Egr3* and D2-MSN-specific induction of *Egr3* successfully blunted cocaine driven behaviors (Chandra et al., 2015; Engeln et al., 2020). Our Cre-dependent CRISPR tools afford the ability to manipulate MSN subtypes for *in vivo* gene perturbation studies to elucidate D1- or D2-MSN *Egr3* and *Nab2* dynamics in the intact brain in the future studies.

Altered histone methylation, and corresponding histone-modifying enzymes, occur in NAc and other reward-related brain regions with exposure to psychostimulants (Maze et al., 2010; Robison and Nestler, 2011; Aguilar-Valles et al., 2014; Heller et al., 2016). Genetic and pharmacological interventions of

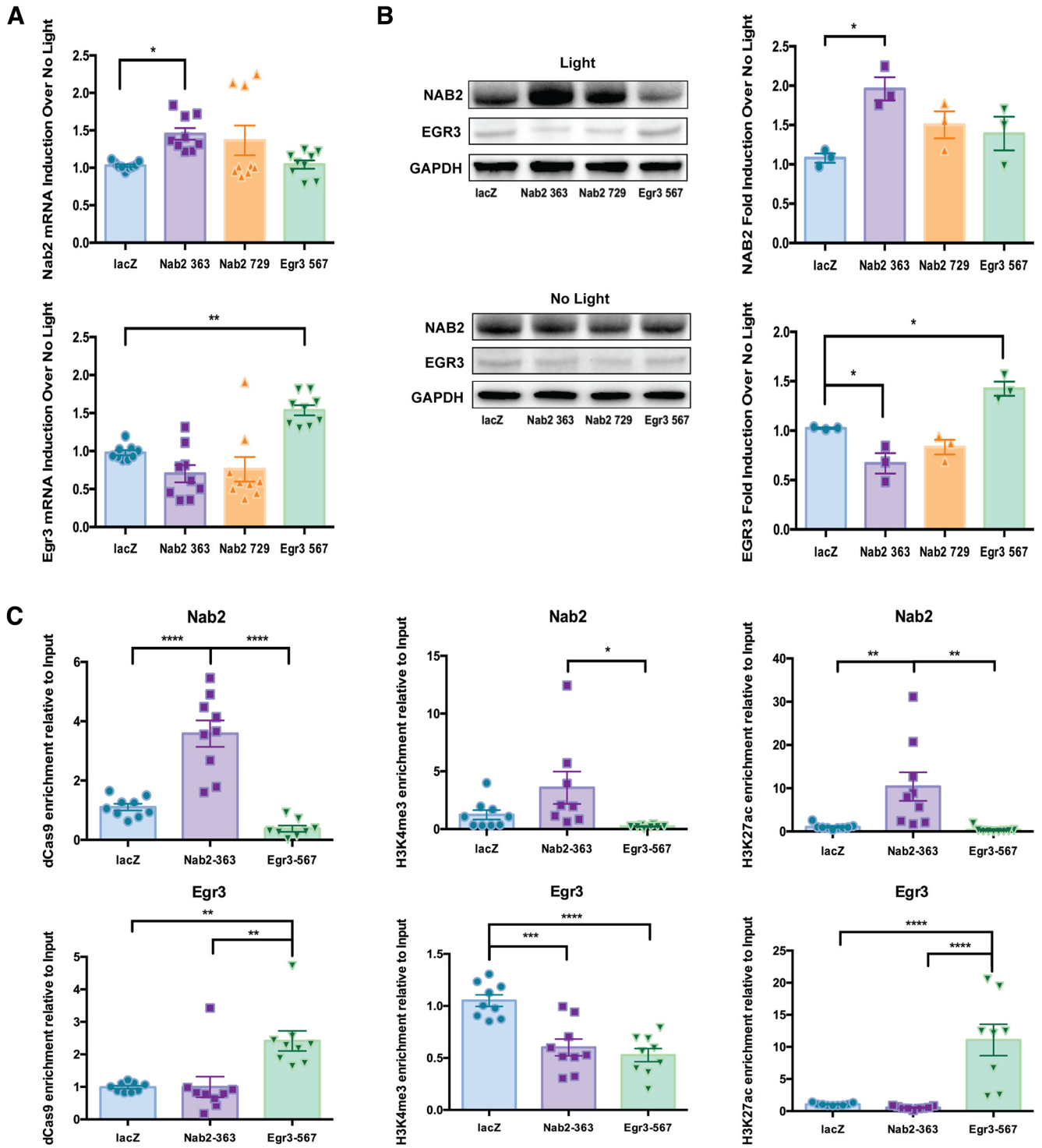

Figure 8. Opto-CRISPR-p300-mediated activation of *Nab2* and *Egr3* transcription. ***A***, qRT-PCR demonstrates that 2 h of blue light stimulation induced *Nab2* mRNA and *Egr3* mRNA expression in cells transfected with *Nab2* or *Egr3* sgRNAs, respectively, and Opto-CRISPR-p300 ($n = 9$ per condition). ***B***, Western blots demonstrate that 2 h of blue light stimulation induced NAB2 levels while downregulating EGR3 levels in cells transfected with Opto-CRISPR-p300 and *Nab2* sgRNA. EGR3 levels were upregulated, while NAB2 levels were unchanged in cells transfected with Opto-CRISPR-p300 and *Egr3* sgRNA ($n = 3$ per condition). ***C***, Cut&Run of blue light-stimulated Neuro2a cells transfected with Opto-CRISPR-p300 display enrichment of Opto-CRISPR-p300 complex on the promoters of respective genes targeted by sgRNAs compared with lacZ sgRNA controls. Transcriptional activation marks, H3K4me3 and H3K27ac, have increased enrichment on the promoters of respective genes targeted by sgRNAs compared with lacZ sgRNA controls ($n = 9$ per condition). Error bar indicates mean ± SEM. $^{*}p < 0.05$. $^{**}p < 0.01$. $^{***}p < 0.001$. $^{****}p < 0.0001$.

histone-modifying enzymes in NAc and other reward-related brain regions during drug-mediated behaviors shed light on epigenetic regulations and corresponding gene regulations. However, many of these studies examine global regulation of histone-modifying enzymes rather than regulation at specific loci, although some recent studies examine loci specific manipulations (Carpenter et al., 2020; Xu et al., 2021). Furthermore, many of these studies examine bulk tissue alterations rather

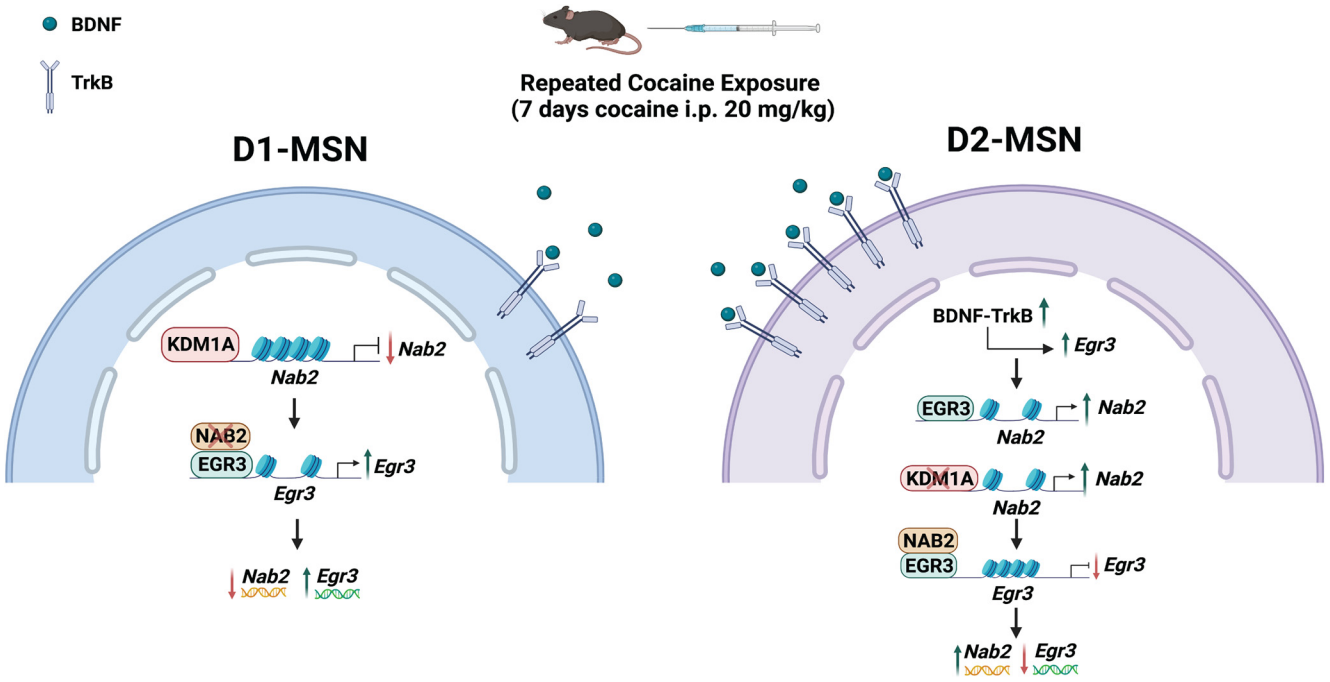

Figure 9. Proposed model of Nab2 and Egr3 regulation after repeated exposure to cocaine. Nab2 expression is decreased and Egr3 expression is increased in NAc D1-MSNs after repeated exposure to cocaine. Oppositely, Nab2 expression is increased and Egr3 expression is decreased in NAc D2-MSNs after repeated exposure to cocaine.

than cell type-specific changes. In our findings, we observed bidirectional induction of *Kdm1a* and *Kdm6a* in D1- and D2-MSNs after repeated cocaine. In contrast, *Kdm5c* was only induced in D2-MSNs, while *Kdm4a* did not show a change in either subtype. The expression of *Kdm6a* in the PFC was reported to be downregulated in rat cocaine self-administration studies (Sadakierska-Chudy et al., 2017). These changes in *Kdm*s may occur through cocaine-induced dopamine receptor signaling cascades. Previous studies showed cocaine-mediated D1 activation may cause imbalance of H3K4me3/H3K27me3 via downregulation of *Kdm1a* (González et al., 2020). These cell subtype-specific regulation of *Kdm*s may drive the imbalance of MSN subtype epigenome regulation with repeated cocaine, with impact on the transcriptional landscape to promote cellular and behavioral adaptations occurring with cocaine exposure.

Our findings showing bidirectional regulation of *Kdm1a* in NAc cell subtypes after repeated cocaine exposure emphasize the importance of examining *Kdm1a* regulation of *Egr3* and *Nab2* transcription. Using our Cre- and blue light-inducible Opto-CRISPR-KDM1A system to target KDM1A to the *Nab2* promoter, we observed reduced expression of *Nab2* while inducing *Egr3* expression in Neuro2a cells. Similarly, targeting the *Egr3* promoter resulted in reduced expression of *Egr3* while inducing *Nab2* expression. Previous studies demonstrated that *Kdm1a* acts on H3K4 and H3K9 to demethylate these histone modifications (Shi et al., 2004; Forneris et al., 2005; Metzger et al., 2005; Garcia-Bassets et al., 2007; Nair et al., 2010; Rudolph et al., 2013). *Kdm1a* functions to both repress and activate transcription by mediating histone H3K4me1/2 and H3K9me1/2 demethylation, respectively. Our findings show that Opto-CRISPR-KDM1A causes repression of both *Egr3* and *Nab2* and likely targets H3K4 at their promoters. However, it is plausible that sgRNA targeting at different promoter regions or other genes could result in Opto-CRISPR-KDM1A demethylating H3K9 to induce transcription. Replacing the KDM1A with truncated core of p300 histone acetyltransferase allowed us to engineer a Opto-CRISPR-p300 system for Cre- and light-inducible activation of target genes. Targeting *Nab2* with Opto-CRISPR-p300 induced the expression of *Nab2* while reducing *Egr3*. In contrast, targeting *Egr3* with Opto-CRISPR-p300 induced the expression of *Egr3* and blunted *Nab2* expression in Neuro2a cells. This is consistent with previous findings demonstrating dCas9-fused catalytic core region of p300 is sufficient to drive the transcription of its target (Hilton et al., 2015) and consistent with the role of p300 targeting acetylation to promote transcription. Acetylation of H3K27 mark is one of the most widely studied indicators of enhancer activity (Ogryzko et al., 1996; Chen and Li, 2011; Delvecchio et al., 2013). Not surprisingly, enrichment of H3K27ac on the promoters of *Egr3* and *Nab2*, when Opto-CRISPR-p300 is targeted with *Egr3* or *Nab2* sgRNA, respectively, is also consistent with endogenous p300 binding profiles (Visel et al., 2009; Rada-Iglesias et al., 2011).

In recent years, CRISPR tools emerged as potent methods for genetic perturbation and epigenetic editing (Dominguez et al., 2016; Yeo et al., 2018; Zheng et al., 2018; Savell et al., 2019; Duke et al., 2020; Carullo et al., 2021). These tools offer considerable merit over the traditional methods for gene silencing and overexpression in sequence-dependent and sequence-independent off-target specificity (Bridge et al., 2003; Jackson et al., 2003; Sledz et al., 2003; Khan et al., 2009; Olejniczak et al., 2016). Since dCas9-KRAB- and dCas9-VP64-mediated genetic perturbations can be achieved in a cell type-specific manner, these tools would have a broad appeal for studies that aim to decipher cell type-specific questions. Our Opto-CRISPR tools allow cell type and light-inducible spatiotemporally precise manipulations which may mimic more endogenous expression patterns and allow precise control of the duration of gene perturbation as well as reversible manipulations once the light stimulation has been turned off. *In vivo* applications of these Opto-CRISPR tools would allow an array of molecular and behavioral experiments far beyond the scope of this study. This includes temporal studies where transcriptional manipulation of a target gene can be modulated at different time points during the course of

the drug exposure or abstinence. They may also permit the fine control over the degree of gene transcription by the ability to ramp up or down transcription with light. Importantly, the optical inducibility allows the manipulation to be reversible.

Our findings demonstrate novel and dynamic regulation of *Nab2* and *Egr3* in NAc MSN subtypes with cocaine exposure and demonstrate the ability to use CRISPR epigenome editing tools to explore this regulation. The synthetic epigenetic manipulation of histone profiles and downstream transcription is critical in deciphering complex psychostimulant-induced changes in the molecular landscape. The versatility of these Cre- and light-inducible Opto-CRISPR tool sets allow the study of specific cell type transcriptional profiles after cocaine and other conditions. Importantly, such tools can be applied in future studies for specific manipulation of transcriptional profiles that are critical for psychostimulant-induced cellular and behavioral plasticity and with spatiotemporal precision. These results emphasize the need for detailed elucidation of transcriptional underpinnings at cell type-specific resolution and CRISPRi/CRISPRa constructs allow physiologically relevant manipulations of transcripts to explore molecular substrates occurring in models of cocaine use disorder.

References

Aguilar-Valles A, Vaissière T, Griggs EM, Mikaelsson MA, Takács IF, Young EJ, Rumbaugh G, Miller CA (2014) Methamphetamine-associated memory is regulated by a writer and an eraser of permissive histone methylation. Biol Psychiatry 76:57–65.

Arango-Lievano M, Schwarz JT, Vernov M, Wilkinson MB, Bradbury K, Feliz A, Marongiu R, Gelfand Y, Warner-Schmidt J, Nestler EJ, Greengard P, Russo SJ, Kaplitt MG (2014) Cell type-specific expression of p11 controls cocaine reward. Biol Psychiatry 76:794–801.

Basta J, Rauchman M (2015) The nucleosome remodeling and deacetylase complex in development and disease. Transl Res 165:36–47.

Bateup HS, Svenningsson P, Kuroiwa M, Gong S, Nishi A, Heintz N, Greengard P (2008) Cell type-specific regulation of DARPP-32 phosphorylation by psychostimulant and antipsychotic drugs. Nat Neurosci 11:932–939.

Bateup HS, Santini E, Shen W, Birnbaum S, Valjent E, Surmeier DJ, Fisone G, Nestler EJ, Greengard P (2010) Distinct subclasses of medium spiny neurons differentially regulate striatal motor behaviors. Proc Natl Acad Sci USA 107:14845–14850.

Beckmann AM, Wilce PA (1997) Egr transcription factors in the nervous system. Neurochem Int 31:477–510.

Bock R, Hoon Shin J, Kaplan AR, Dobi A, Markey E, Kramer PF, Gremel CM, Christensen CH, Adrover MF, Alvarez VA (2013) Strengthening the accumbal indirect pathway promotes resilience to compulsive cocaine use. Nat Neurosci 16:632–638.

Bridge AJ, Pebernard S, Ducraux A, Nicoulaz AL, Iggo R (2003) Induction of an interferon response by RNAi vectors in mammalian cells. Nat Genet 34:263–264.

Carlezon WA, Duman RS, Nestler EJ (2005) The many faces of CREB. Trends Neurosci 28:436–445.

Carpenter MD, Hu Q, Bond AM, Lombroso SI, Czarnecki KS, Lim CJ, Song H, Wimmer ME, Pierce RC, Heller EA (2020) Nr4a1 suppresses cocaine-induced behavior via epigenetic regulation of homeostatic target genes. Nat Commun 11:504.

Carter JH, Lefebvre JM, Wiest DL, Tourtellotte WG (2007) Redundant role for early growth response transcriptional regulators in thymocyte differentiation and survival. J Immunol 178:6796–6805.

Carullo NV, Hinds JE, Revanna JS, Tuscher JJ, Bauman AJ, Day JJ (2021) A Cre-dependent CRISPR/dCas9 system for gene expression regulation in neurons. eNeuro 8:ENEURO.0188-21.2021.

Chandra R, Lenz J, Gancarz AM, Chaudhury D, Schroeder GL, Han MH, Cheer JF, Dietz DM, Kay Lobo M (2013) Optogenetic inhibition of D1R containing nucleus accumbens neurons alters cocaine-mediated regulation of Tiam1. Front Mol Neurosci 6:13.

Chandra R, Chase Francis T, Konkalmatt P, Amgalan A, Gancarz AM, Dietz DM, Lobo MK (2015) Opposing role for Egr3 in nucleus accumbens cell subtypes in cocaine action. J Neurosci 35:7927–7937.

Chandra R, et al. (2017a) Drp1 mitochondrial fission in D1 neurons mediates behavioral and cellular plasticity during early cocaine abstinence. Neuron 96:1327–1341.e6.

Chandra R, Engeln M, Francis TC, Konkalmatt P, Patel D, Lobo MK (2017b) A role for peroxisome proliferator-activated receptor gamma coactivator-1α in nucleus accumbens neuron subtypes in cocaine action. Biol Psychiatry 81:564–572.

Chandwani S, Keilani S, Ortiz-Virumbrales M, Morant A, Bezdecny S, Ehrlich ME (2013) Induction of DARPP-32 by brain-derived neurotrophic factor in striatal neurons in vitro is modified by histone deacetylase inhibitors and Nab2. PLoS One 8:e76842.

Chen J, Li Q (2011) Life and death of transcriptional co-activator p300. Epigenetics 6:957–961.

Cole SL, Chandra R, Harris M, Patel I, Wang T, Kim H, Jensen L, Russo SJ, Turecki G, Gancarz-Kausch AM, Dietz DM, Lobo MK (2021) Cocaine-induced neuron subtype mitochondrial dynamics through Egr3 transcriptional regulation. Mol Brain 14:101.

Collins S, Lutz MA, Zarek PE, Anders RA, Kersh GJ, Powell JD (2008) Opposing regulation of T cell function by Egr-1/NAB2 and Egr-2/Egr-3. Eur J Immunol 38:528–536.

Creyghton MP, Cheng AW, Welstead GG, Kooistra T, Carey BW, Steine EJ, Hanna J, Lodato MA, Frampton GM, Sharp PA, Boyer LA, Young RA, Jaenisch R (2010) Histone H3K27ac separates active from poised enhancers and predicts developmental state. Proc Natl Acad Sci USA 107:21931–21936.

Delvecchio M, Gaucher J, Aguilar-Gurrieri C, Ortega E, Panne D (2013) Structure of the p300 catalytic core and implications for chromatin targeting and HAT regulation. Nat Struct Mol Biol 20:1040–1046.

Di Chiara G (2002) Nucleus accumbens shell and core dopamine: differential role in behavior and addiction. Behav Brain Res 137:75–114.

Dominguez AA, Lim WA, Qi LS (2016) Beyond editing: repurposing CRISPR-Cas9 for precision genome regulation and interrogation. Nat Rev Mol Cell Biol 17:5–15.

Duke CG, Savell KE, Tuscher JJ, Phillips RA, Day JJ (2019) Blue light-induced gene expression alterations in cultured neurons are the result of phototoxic interactions with neuronal culture media. eNeuro 7:ENEURO.0386-19.2019.

Duke CG, Bach SV, Revanna JS, Sultan FA, Southern NT, Davis MN, Carullo NV, Bauman AJ, Phillips RA, Day JJ (2020) An improved CRISPR/dCas9 interference tool for neuronal gene suppression. Front Genome Ed 2:9.

Eagle AL, Manning CE, Williams ES, Bastle RM, Gajewski PA, Garrison A, Wirtz AJ, Akguen S, Brandel-Ankrapp K, Endege W, Boyce FM, Ohnishi YN, Mazei-Robison M, Maze I, Neve RL, Robison AJ (2020) Circuit-specific hippocampal ΔFosB underlies resilience to stress-induced social avoidance. Nat Commun 11:4484.

Ena SL, De Backer JF, Schiffmann SN, de Kerchove d'Exaerde A (2013) FACS array profiling identifies ecto-5′nucleotidase as a striatopallidal neuron-specific gene involved in striatal-dependent learning. J Neurosci 33:8794–8809.

Engeln M, Mitra S, Chandra R, Gyawali U, Fox ME, Dietz DM, Lobo MK (2020) Sex-specific role for Egr3 in nucleus accumbens D2-medium spiny neurons following long-term abstinence from cocaine self-administration. Biol Psychiatry 87:992–1000.

Engeln M, Fox ME, Chandra R, Choi EY, Nam H, Qadir H, Thomas SS, Rhodes VM, Turner MD, Herman RJ, Calarco CA, Lobo MK (2022) Transcriptome profiling of the ventral pallidum reveals a role for pallidothalamic neurons in cocaine reward. Mol Psychiatry 27:3980–3991.

Farhang N, Brunger JM, Stover JD, Thakore PI, Lawrence B, Guilak F, Gersbach CA, Setton LA, Bowles RD (2017) CRISPR-based epigenome editing of cytokine receptors for the promotion of cell survival and tissue deposition in inflammatory environments. Tissue Eng Part A 23:738–749.

Feng J, Wilkinson M, Liu X, Purushothaman I, Ferguson D, Vialou V, Maze I, Shao N, Kennedy P, Koo J, Dias C, Laitman B, Stockman V, LaPlant Q, Cahill ME, Nestler EJ, Shen L (2014) Chronic cocaine-regulated epigenomic changes in mouse nucleus accumbens. Genome Biol 15:R65.

Ferguson SM, Eskenazi D, Ishikawa M, Wanat MJ, Phillips PE, Dong Y, Roth BL, Neumaier JF (2011) Transient neuronal inhibition reveals opposing

roles of indirect and direct pathways in sensitization. Nat Neurosci 14:22–24.
Ferrari KJ, Scelfo A, Jammula S, Cuomo A, Barozzi I, Stützer A, Fischle W, Bonaldi T, Pasini D (2014) Polycomb-dependent H3K27me1 and H3K27me2 regulate active transcription and enhancer fidelity. Mol Cell 53:49–62.
Forneris F, Binda C, Vanoni MA, Battaglioli E, Mattevi A (2005) Human histone demethylase LSD1 reads the histone code. J Biol Chem 280:41360–41365.
Garcia-Bassets I, Kwon YS, Telese F, Prefontaine GG, Hutt KR, Cheng CS, Ju BG, Ohgi KA, Wang J, Escoubet-Lozach L, Rose DW, Glass CK, Fu XD, Rosenfeld MG (2007) Histone methylation-dependent mechanisms impose ligand dependency for gene activation by nuclear receptors. Cell 128:505–518.
Gerfen CR, Engber TM, Mahan LC, Susel Z, Chase TN, Monsma FJ, Sibley DR (1990) D1 and D2 dopamine receptor-regulated gene expression of striatonigral and striatopallidal neurons. Science 250:1429–1432.
Gerfen CR, Paletzki R, Heintz N (2013) GENSAT BAC cre-recombinase driver lines to study the functional organization of cerebral cortical and basal ganglia circuits. Neuron 80:1368–1383.
Gerhardt KP, Olson EJ, Castillo-Hair SM, Hartsough LA, Landry BP, Ekness F, Yokoo R, Gomez EJ, Ramakrishnan P, Suh J, Savage DF, Tabor JJ (2016) An open-hardware platform for optogenetics and photobiology. Sci Rep 6:35363.
Gong S, Doughty M, Harbaugh CR, Cummins A, Hatten ME, Heintz N, Gerfen CR (2007) Targeting Cre recombinase to specific neuron populations with bacterial artificial chromosome constructs. J Neurosci 27:9817–9823.
González B, Gancedo SN, Garazatua SA, Roldán E, Vitullo AD, González CR (2020) Dopamine receptor D1 contributes to cocaine epigenetic reprogramming of histone modifications in male germ cells. Front Cell Dev Biol 8:216.
Heiman M, Schaefer A, Gong S, Peterson JD, Day M, Ramsey KE, Suárez-Fariñas M, Schwarz C, Stephan DA, Surmeier DJ, Greengard P, Heintz N (2008) A translational profiling approach for the molecular characterization of CNS cell types. Cell 135:738–748.
Heintzman ND, et al. (2009) Histone modifications at human enhancers reflect global cell-type-specific gene expression. Nature 459:108–112.
Heintzman ND, Stuart RK, Hon G, Fu Y, Ching CW, Hawkins RD, Barrera LO, Van Calcar S, Qu C, Ching KA, Wang W, Weng Z, Green RD, Crawford GE, Ren B (2007) Distinct and predictive chromatin signatures of transcriptional promoters and enhancers in the human genome. Nat Genet 39:311–318.
Heller EA, et al. (2014) Locus-specific epigenetic remodeling controls addiction- and depression-related behaviors. Nat Neurosci 17:1720–1727.
Heller EA, Hamilton PJ, Burek DD, Lombroso SI, Peña CJ, Neve RL, Nestler EJ (2016) Targeted epigenetic remodeling of the Cdk5 gene in nucleus accumbens regulates cocaine- and stress-evoked behavior. J Neurosci 36:4690–4697.
Hikida T, Kimura K, Wada N, Funabiki K, Nakanishi Shigetada S (2010) Distinct roles of synaptic transmission in direct and indirect striatal pathways to reward and aversive behavior. Neuron 66:896–907.
Hilton IB, D'Ippolito AM, Vockley CM, Thakore PI, Crawford GE, Reddy TE, Gersbach CA (2015) Epigenome editing by a CRISPR-Cas9-based acetyltransferase activates genes from promoters and enhancers. Nat Biotechnol 33:510–517.
Honkaniemi J, Zhang JS, Longo FM, Sharp FR (2000) Stress induces zinc finger immediate early genes in the rat adrenal gland. Brain Res 877:203–208.
Hughes RM, Bolger S, Tapadia H, Tucker CL (2012) Light-mediated control of DNA transcription in yeast. Methods 58:385–391.
Hyman SE, Malenka RC, Nestler EJ (2006) Neural mechanisms of addiction: the role of reward-related learning and memory. Annu Rev Neurosci 29:565–598.
Jackson AL, Bartz SR, Schelter J, Kobayashi SV, Burchard J, Mao M, Li B, Cavet G, Linsley PS (2003) Expression profiling reveals off-target gene regulation by RNAi. Nat Biotechnol 21:635–637.
Jouvert P, Dietrich JB, Aunis D, Zwiller J (2002) Differential rat brain expression of EGR proteins and of the transcriptional corepressor NAB in response to acute or chronic cocaine administration. Neuromolecular Med 1:137–151.
Kennedy MJ, Hughes RM, Peteya LA, Schwartz JW, Ehlers MD, Tucker CL (2010) Rapid blue-light-mediated induction of protein interactions in living cells. Nat Methods 7:973–975.
Khan AA, Betel D, Miller ML, Sander C, Leslie CS, Marks DS (2009) Transfection of small RNAs globally perturbs gene regulation by endogenous microRNAs. Nat Biotechnol 27:549–555.
Kim J, Park BH, Lee JH, Park SK, Kim JH (2011) Cell type-specific alterations in the nucleus accumbens by repeated exposures to cocaine. Biol Psychiatry 69:1026–1034.
Kim J, Roberts DS, Hu Y, Lau GC, Brooks-Kayal AR, Farb DH, Russek SJ (2012) Brain-derived neurotrophic factor uses CREB and Egr3 to regulate NMDA receptor levels in cortical neurons. J Neurochem 120:210–219.
Klann TS, Black JB, Chellappan M, Safi A, Song L, Hilton IB, Crawford GE, Reddy TE, Gersbach CA (2017) CRISPR-Cas9 epigenome editing enables high-throughput screening for functional regulatory elements in the human genome. Nat Biotechnol 35:561–568.
Konermann S, Brigham MD, Trevino AE, Hsu PD, Heidenreich M, Cong L, Platt RJ, Scott DA, Church GM, Zhang F (2013) Optical control of mammalian endogenous transcription and epigenetic states. Nature 500:472–476.
Kumbrink J, Gerlinger M, Johnson JP (2005) Egr-1 induces the expression of its corepressor Nab2 by activation of the Nab2 promoter thereby establishing a negative feedback loop. J Biol Chem 280:42785–42793.
Kumbrink J, Kirsch KH, Johnson JP (2010) EGR1, EGR2, and EGR3 activate the expression of their coregulator NAB2 establishing a negative feedback loop in cells of neuroectodermal and epithelial origin. J Cell Biochem 111:207–217.
Lee KW, Kim Y, Kim AM, Helmin K, Nairn AC, Greengard P (2006) Cocaine-induced dendritic spine formation in D1 and D2 dopamine receptor-containing medium spiny neurons in nucleus accumbens. Proc Natl Acad Sci USA 103:3399–3404.
Lenz JD, Lobo MK (2013) Optogenetic insights into striatal function and behavior. Behav Brain Res 255:44–54.
Lobo MK, Nestler EJ (2011) The striatal balancing act in drug addiction: distinct roles of direct and indirect pathway medium spiny neurons. Front Neuroanat 5:41.
Lobo MK, Karsten SL, Gray M, Geschwind DH, Yang XW (2006) FACS-array profiling of striatal projection neuron subtypes in juvenile and adult mouse brains. Nat Neurosci 9:443–452.
Lobo MK, Covington HE, Chaudhury D, Friedman AK, Sun HS, Damez-Werno D, Dietz DM, Zaman S, Koo JW, Kennedy PJ, Mouzon E, Mogri M, Neve RL, Deisseroth K, Han MH, Nestler EJ (2010) Cell type-specific loss of BDNF signaling mimics optogenetic control of cocaine reward. Science 330:385–390.
Lobo MK, et al. (2013) ΔFosB induction in striatal medium spiny neuron subtypes in response to chronic pharmacological, emotional, and optogenetic stimuli. J Neurosci 33:18381–18395.
Maze I, Covington HE, Dietz DM, LaPlant Q, Renthal W, Russo SJ, Mechanic M, Mouzon E, Neve RL, Haggarty SJ, Ren Y, Sampath SC, Hurd YL, Greengard P, Tarakhovsky A, Schaefer A, Nestler EJ (2010) Essential role of the histone methyltransferase G9a in cocaine-induced plasticity. Science 327:213–216.
Maze I, Chaudhury D, Dietz DM, Von Schimmelmann M, Kennedy PJ, Lobo MK, Sillivan SE, Miller ML, Bagot RC, Sun HS, Turecki G, Neve RL, Hurd YL, Shen L, Han MH, Schaefer A, Nestler EJ (2014) G9a influences neuronal subtype-specification in striatum. Nat Neurosci 17:533–539.
McGinty JF, Whitfield TW, Berglind WJ (2010) Brain-derived neurotrophic factor and cocaine addiction. Brain Res 1314:183–193.
Metzger E, Wissmann M, Yin N, Müller JM, Schneider R, Peters AH, Günther T, Buettner R, Schüle R (2005) LSD1 demethylates repressive histone marks to promote androgen-receptor-dependent transcription. Nature 437:436–439.
Nair SS, Nair BC, Cortez V, Chakravarty D, Metzger E, Schüle R, Brann DW, Tekmal RR, Vadlamudi RK (2010) PELP1 is a reader of histone H3 methylation that facilitates oestrogen receptor-alpha target gene activation by regulating lysine demethylase 1 specificity. EMBO Rep 11:438–444.
Nestler EJ (2014) Epigenetic mechanisms of drug addiction. Neuropharmacology 76:259–268.
Nihongaki Y, Kawano F, Nakajima T, Sato M (2015) Photoactivatable CRISPR-Cas9 for optogenetic genome editing. Nat Biotechnol 33:755–760.

O'Donovan KJ, Baraban JM (1999) Major Egr3 isoforms are generated via alternate translation start sites and differ in their abilities to activate transcription. Mol Cell Biol 19:4711–4718.
Ogryzko VV, Schiltz RL, Russanova V, Howard BH, Nakatani Y (1996) The transcriptional coactivators p300 and CBP are histone acetyltransferases. Cell 87:953–959.
Olejniczak M, Urbanek MO, Jaworska E, Witucki L, Szczesniak MW, Makalowska I, Krzyzosiak WJ (2016) Sequence-non-specific effects generated by various types of RNA interference triggers. Biochim Biophys Acta 1859:306–314.
Patwardhan S, Gashler A, Siegel MG, Chang LC, Joseph LJ, Shows TB, Le Beau MM, Sukhatme VP (1991) EGR3, a novel member of the Egr family of genes encoding immediate-early transcription factors. Oncogene 6:917–928.
Polstein LR, Gersbach CA (2015) A light-inducible CRISPR-Cas9 system for control of endogenous gene activation. Nat Chem Biol 11:198–200.
Qi LS, Larson MH, Gilbert LA, Doudna JA, Weissman JS, Arkin AP, Lim WA (2013) Repurposing CRISPR as an RNA-guided platform for sequence-specific control of gene expression. Cell 152:1173–1183.
Rada-Iglesias A, Bajpai R, Swigut T, Brugmann SA, Flynn RA, Wysocka J (2011) A unique chromatin signature uncovers early developmental enhancers in humans. Nature 470:279–283.
Ran FA, Cong L, Yan WX, Scott DA, Gootenberg JS, Kriz AJ, Zetsche B, Shalem O, Wu X, Makarova KS, Koonin EV, Sharp PA, Zhang F (2015) In vivo genome editing using *Staphylococcus aureus* Cas9. Nature 520:186–191.
Roberts DS, Hu Y, Lund IV, Brooks-Kayal AR, Russek SJ (2006) Brain-derived neurotrophic factor (BDNF)-induced synthesis of early growth response factor 3 (Egr3) controls the levels of type A GABA receptor alpha 4 subunits in hippocampal neurons. J Biol Chem 281:29431–29435.
Robison AJ, Nestler EJ (2011) Transcriptional and epigenetic mechanisms of addiction. Nat Rev Neurosci 12:623–637.
Rothwell PE, Fuccillo MV, Maxeiner S, Hayton SJ, Gokce O, Lim BK, Fowler SC, Malenka RC, Südhof TC (2014) Autism-associated neuroligin-3 mutations commonly impair striatal circuits to boost repetitive behaviors. Cell 158:198–212.
Rudolph T, Beuch S, Reuter G (2013) Lysine-specific histone demethylase LSD1 and the dynamic control of chromatin. Biol Chem 394:1019–1028.
Russo SJ, et al. (2009) Nuclear factor kappa B signaling regulates neuronal morphology and cocaine reward. J Neurosci 29:3529–3537.
Russo SJ, Dietz DM, Dumitriu D, Morrison JH, Malenka RC, Nestler EJ (2010) The addicted synapse: mechanisms of synaptic and structural plasticity in nucleus accumbens. Trends Neurosci 33:267–276.
Russo SJ, Nestler EJ (2013) The brain reward circuitry in mood disorders. Nat Rev Neurosci 14:609–625.
Sadakierska-Chudy A, Frankowska M, Miszkiel J, Wydra K, Jastrzębska J, Filip M (2017) Prolonged induction of miR-212/132 and REST expression in rat striatum following cocaine self-administration. Mol Neurobiol 54:2241–2254.
Salgado S, Kaplitt MG (2015) The nucleus accumbens: a comprehensive review. Stereotact Funct Neurosurg 93:75–93.
Sanz E, Evanoff R, Quintana A, Evans E, Miller JA, Ko C, Amieux PS, Griswold MD, McKnight GS (2013) RiboTag analysis of actively translated mRNAs in Sertoli and Leydig cells in vivo. PLoS One 8:e66179.
Sanz E, Yang L, Su T, Morris DR, McKnight GS, Amieux PS (2009) Cell-type-specific isolation of ribosome-associated mRNA from complex tissues. Proc Natl Acad Sci USA 106:13939–13944.
Savell KE, Bach SV, Zipperly ME, Revanna JS, Goska NA, Tuscher JJ, Duke CG, Sultan FA, Burke JN, Williams D, Ianov L, Day JJ (2019) A neuron-optimized CRISPR/dCas9 activation system for robust and specific gene regulation. eNeuro 6:ENEURO.0495-18.2019.
Shi Y, Lan F, Matson C, Mulligan P, Whetstine JR, Cole PA, Casero RA, Shi Y (2004) Histone demethylation mediated by the nuclear amine oxidase homolog LSD1. Cell 119:941–953.
Skene PJ, Henikoff S (2017) An efficient targeted nuclease strategy for high-resolution mapping of DNA binding sites. Elife 6:e21856.
Sledz CA, Holko M, de Veer MJ, Silverman RH, Williams BR (2003) Activation of the interferon system by short-interfering RNAs. Nat Cell Biol 5:834–839.
Smith RJ, Lobo MK, Spencer S, Kalivas PW (2013) Cocaine-induced adaptations in D1 and D2 accumbens projection neurons (a dichotomy not necessarily synonymous with direct and indirect pathways). Curr Opin Neurobiol 23:546–552.
Suehiro J, Hamakubo T, Kodama T, Aird WC, Minami T (2010) Vascular endothelial growth factor activation of endothelial cells is mediated by early growth response-3. Blood 115:2520–2532.
Surmeier DJ, Ding J, Day M, Wang Z, Shen W (2007) D1 and D2 dopamine-receptor modulation of striatal glutamatergic signaling in striatal medium spiny neurons. Trends Neurosci 30:228–235.
Taslimi A, Zoltowski B, Miranda JG, Pathak GP, Hughes RM, Tucker CL (2016) Optimized second-generation CRY2-CIB dimerizers and photoactivatable Cre recombinase. Nat Chem Biol 12:425–430.
Teague CD, et al. (2022) CREB binding at the Zfp189 promoter within medium spiny neuron subtypes differentially regulates behavioral and physiological adaptations over the course of cocaine use. Biol Psychiatry Advance online publication. Retrieved Aug. 5, 2022. https://doi.org/10.1016/j.biopsych.2022.07.022.
Thiel G, Cibelli G (2002) Regulation of life and death by the zinc finger transcription factor Egr-1. J Cell Physiol 193:287–292.
Unoki M, Nakamura Y (2003) EGR2 induces apoptosis in various cancer cell lines by direct transactivation of BNIP3L and BAK. Oncogene 22:2172–2185.
Visel A, Blow MJ, Li Z, Zhang T, Akiyama JA, Holt A, Plajzer-Frick I, Shoukry M, Wright C, Chen F, Afzal V, Ren B, Rubin EM, Pennacchio LA (2009) ChIP-seq accurately predicts tissue-specific activity of enhancers. Nature 457:854–858.
Volkow ND, Fowler JS, Wang GJ, Baler R, Telang F (2009) Imaging dopamine's role in drug abuse and addiction. Neuropharmacology 56:3–8.
Wang Y, Zhang H, Chen Y, Sun Y, Yang F, Yu W, Liang J, Sun L, Yang X, Shi L, Li R, Li Y, Zhang Y, Li Q, Yi X, Shang Y (2009) LSD1 is a subunit of the NuRD complex and targets the metastasis programs in breast cancer. Cell 138:660–672.
Wang Z, Zang C, Rosenfeld JA, Schones DE, Barski A, Cuddapah S, Cui K, Roh TY, Peng W, Zhang MQ, Zhao K (2008) Combinatorial patterns of histone acetylations and methylations in the human genome. Nat Genet 40:897–903.
Wise RA (2004) Dopamine, learning and motivation. Nat Rev Neurosci 5:483–494.
Wysocka J, Swigut T, Xiao H, Milne TA, Kwon SY, Landry J, Kauer M, Tackett AJ, Chait BT, Badenhorst P, Wu C, Allis CD (2006) A PHD finger of NURF couples histone H3 lysine 4 trimethylation with chromatin remodelling. Nature 442:86–90.
Xu SJ, Lombroso SI, Fischer DK, Carpenter MD, Marchione DM, Hamilton PJ, Lim CJ, Neve RL, Garcia BA, Wimmer ME, Pierce RC, Heller EA (2021) Chromatin-mediated alternative splicing regulates cocaine-reward behavior. Neuron 109:2943–2966.e8.
Yamagata K, Kaufmann WE, Lanahan A, Papapavlou M, Barnes CA, Andreasson KI, Worley PF (1994) Egr3/Pilot, a zinc finger transcription factor, is rapidly regulated by activity in brain neurons and colocalizes with Egr1/zif268. Learn Mem 1:140–152.
Yeo NC, et al. (2018) An enhanced CRISPR repressor for targeted mammalian gene regulation. Nat Methods 15:611–616.
Zheng Y, Shen W, Zhang J, Yang B, Liu YN, Qi H, Yu X, Lu SY, Chen Y, Xu YZ, Li Y, Gage FH, Mi S, Yao J (2018) CRISPR interference-based specific and efficient gene inactivation in the brain. Nat Neurosci 21:447–454.